

Development of Targeted Diagnostic and Therapeutic Tools for Detection and Treatment of Oligodendrogliomas

M.Sc. Thesis

by

Aishi Chakrabarti



**DISCIPLINE OF CHEMISTRY
INDIAN INSTITUTE OF TECHNOLOGY INDORE
JUNE 2020**

Development of Targeted Diagnostic and Therapeutic Tools for Detection and Treatment of Oligodendrogliomas

A THESIS

Submitted in partial fulfillment of the requirements for the award of the degree of
Master of Science

by
Aishi Chakrabarti



DISCIPLINE OF CHEMISTRY
INDIAN INSTITUTE OF TECHNOLOGY INDORE
JUNE 2020



INDIAN INSTITUTE OF TECHNOLOGY INDORE

CANDIDATE'S DECLARATION

I hereby certify that the work which is being presented in the thesis entitled **Development of Targeted Diagnostic and Therapeutic tools for Detection and Treatment of Oligodendrogliomas** in the partial fulfillment of the requirements for the award of the degree of **MASTER OF SCIENCE** and submitted in the **DISCIPLINE OF CHEMISTRY, Indian Institute of Technology Indore**, is an authentic record of my own work carried out during the period from July 2019 to June 2020 under the supervision of **Dr. Venkatesh Chelvam**, Associate Professor, IIT Indore.

The matter presented in this thesis has not been submitted by me for the award of any other degree of this or any other institute.

Aishi Chakrabarti
Aishi Chakrabarti

This is to certify that the above statement made by the candidate is correct to the best of my/our knowledge.

Venkatesh C
Dr. Venkatesh Chelvam

Aishi Chakrabarti has successfully given her M.Sc. Oral Examination held on 24th June, 2020

Venkatesh C

Signature of Supervisor of M.Sc. thesis
Date: 11-06-2020

Tushar kanti Mulhosejia

Convener, DPGC
Date: 15-11-2020

Dr. Sanjay Kumar Singh

Signature of PSPC Member
Dr. Sanjay Kumar Singh
Date: 4-11-2020

Dr. Sampak Samanta

Signature of PSPC Member
Dr. Sampak Samanta
Date: 9-11-2020

ACKNOWLEDGEMENTS

I would like to express my gratitude to my supervisor **Dr. Venkatesh Chelvam** for his constant guidance, support, and motivation during my M.Sc. research project. I am thankful for getting the opportunity to work on this project. His enthusiasm and dedication have always inspired me. Further, I would like to thank my PSPC members Dr. Sanjay Kumar Singh and Dr. Sampak Samanta for their valuable suggestions and support.

I would like to express my respect to Prof. Neelesh Kumar Jain (Officiating Director, Indian Institute of Technology Indore) for providing all the facilities at Indian Institute of Technology Indore.

I am also grateful to Dr. Biswarup Pathak (Head, Discipline of Chemistry), Dr. Tridib Kumar Sarma, Dr. Suman Mukhopadhyay, Dr. Apurba Kumar Das, Dr. Sampak Samantha, Dr. Amrendra Kumar Singh, Dr. Anjan Chakraborty, Dr. Tushar Kanti Mukherjee, Dr. Rajneesh Misra and Dr. Satya S. Bulusu for their guidance and help during various activities.

I would like to extend my deep and sincere thanks to my group members Sagnik Sengupta, Ramesh B. Reddy, Amit Pandit, Premansh Dudhe, Srija Tiwari, Mena Asha Krishnan and A V R Krishna Rao for their guidance, encouragement, and support.

I would also like to thank the technical staff from Sophisticated Instrumentation Center (SIC), IIT Indore, Ms. Sarita Batra, Mr. Kinny Pandey, Mr. Ghanshyam Bhavsar and Mr. Manish Kushwaha for their patience and timely technical support without which it was impossible to continue with my work. I would also like to thank Ms. Anjali Bandiwadekar, Mr. Rajesh Kumar, Mr. Lala Ram Ahirwar, and other library staff.

Finally, I would like to express my thanks to IIT Indore and all others who helped and supported me directly or indirectly.

Aishi Chakrabarti

DEDICATION

This thesis is dedicated to my family.....

Abstract

Carbonic anhydrase (CA) IX is an isoform of zinc metalloenzyme CA. It catalyzes the interconversion of carbon dioxide into proton and bicarbonate. CA IX is overexpressed in hypoxic environment due to rapidly proliferating cells. Therefore, it may be considered as a potent biomarker for the detection of various cancers including the brain. In this work, we have synthesized a small molecule ligand attached to a Rhodamine B conjugate as the detection tool. It will also be attached to super paramagnetic iron oxide nanoparticles (SPIONs) for the treatment of oligodendrogliomas using the principle of hyperthermia.

The synthesized bioconjugate consists of three components: a) a small molecule inhibitor specific to the protein of interest (CA IX) b) a peptidic spacer to enhance the distance between targeting ligand and the fluorophore so as to not compromise on the specific binding affinity of the sulfonamide derivative as well as increase the hydrophilicity of the conjugate and c) a fluorophore (Rhodamine B) and a radioisotope chelator for the detection.

TABLE OF CONTENTS

LIST OF FIGURES	x-xi
LIST OF SCHEMES	xii
LIST OF TABLES	xiii
SYMBOLS/UNITS	xv
ACRONYMS	xvii-xviii
Chapter 1: Introduction	1-3
1.1. General introduction	1-2
1.2. Aim of the project	2-3
Chapter 2: Literature	4-5
Chapter 3: Experimental Section	6-15
3.1. Materials and methods	6
3.2. Synthesis of pentafluorobenzene sulfonamide (2)	7
3.3. Synthesis of 3-((2,3,5,6-tetrafluoro - sulfamoylphenyl)thio)propanoic acid (4)	7-8
3.4. Synthesis of 3-((3-(cyclooctylamine)-2,5,6-trifluoro-4- sulfamoylphenyl)thio) propanoic acid (6)	8-9
3.5. Synthesis of CA IX targeted Rhodamine B fluorescent probe (12)	9-11

3.6. Synthesis of CA IX targeted Rhodamine B fluorescent probe (15)	11-12
3.7. Synthesis of CA IX targeted fluorescent and radioimaging probe (22)	12-14
3.8. Synthesis of 3-(2-pyridyldithio)propanoic acid (26)	14-15
3.9. Synthesis of iron oxide nanoparticles (23)	15
3.10. Synthesis of APTES (3-aminopropyl)triethoxy silane) functionalized iron (III) oxide nanoparticles (24)	15
Chapter 4: Results and Discussion	16-24
4.1. Synthesis of small molecule ligand targeting CA IX	16-18
4.2. Synthesis of CA IX targeted Rhodamine B fluorescent probe 12	18-20
4.3. Synthesis of CA IX targeted Rhodamine B fluorescent probe 15	20-21
4.4. Synthesis of CA IX targeted fluorescent and radioimaging probe 22	22-23
4.5. Synthesis of 3-(2-pyridyldithio)propanoic acid 26	23
4.6. Synthesis of functionalized self-immolative disulfide iron oxide nanoparticles 27	24
Chapter 5: Conclusions	25
APPENDIX A	26-35

LIST OF FIGURES

- Figure 1.** ^1H NMR spectrum of pentafluorobenzene sulfonamide **2** in $\text{DMSO-}d_6$ **26**
- Figure 2.** ^{13}C NMR spectrum of pentafluorobenzene sulfonamide **2** in $\text{DMSO-}d_6$ **26**
- Figure 3.** ^{19}F NMR spectrum of pentafluorobenzene sulfonamide **2** in $\text{DMSO-}d_6$ **27**
- Figure 4.** ^1H NMR spectrum of 3-((2,3,5,6-tetrafluoro-4-sulfamoylphenyl)thio)propanoic acid **4** in $\text{DMSO-}d_6$ **27**
- Figure 5.** ^{13}C NMR spectrum of 3-((2,3,5,6-tetrafluoro-4-sulfamoylphenyl)thio)propanoic acid **4** in $\text{DMSO-}d_6$ **28**
- Figure 6.** ^{19}F NMR spectrum of 3-((2,3,5,6-tetrafluoro-4-sulfamoylphenyl)thio)propanoic acid **4** in $\text{DMSO-}d_6$ **28**
- Figure 7.** ^1H NMR spectrum of 3-((3-(cyclooctylamine)-2,5,6-trifluoro-4-sulfamoylphenyl)thio) propanoic acid **6** in $\text{DMSO-}d_6$ **29**
- Figure 8.** ^{13}C NMR spectrum of 3-((3-(cyclooctylamine)-2,5,6-trifluoro-4-sulfamoylphenyl)thio) propanoic acid **6** in $\text{DMSO-}d_6$ **29**
- Figure 9.** ^{19}F NMR spectrum of 3-((3-(cyclooctylamine)-2,5,6-trifluoro-4-sulfamoylphenyl)thio) propanoic acid **6** in $\text{DMSO-}d_6$ in $\text{DMSO-}d_6$ **30**

Figure 10.	¹ H NMR spectrum of 3-(2-pyridyldithio)propionate 26 in CDCl ₃	30
Figure 11.	¹³ C NMR spectrum of 3-(2-pyridyldithio)propionate 26 in CDCl ₃	31
Figure 12.	MS(ESI) of pentafluorobenzenesulfonamide 2	32
Figure 13.	MS(ESI) of 3-((2,3,5,6-tetrafluoro-4-sulfamoylphenyl)thio)propanoic acid 4	32
Figure 14.	MS(ESI) of 3-((3-(cyclooctylamine)-2,5,6-trifluoro-4-sulfamoylphenyl)thio) propanoic acid 6	33
Figure 15.	MS(ESI) of CA IX targeted Rhodamine B fluorescent probe 12	33
Figure 16.	IR spectrum of pentafluorobenzenesulfonamide 2	34
Figure 17.	IR spectrum of 3-((2,3,5,6-tetrafluoro-4-sulfamoylphenyl)thio)propanoic acid 4	34
Figure 18.	IR spectrum of 3-((3-(cyclooctylamine)-2,5,6-trifluoro-4-sulfamoylphenyl)thio) propanoic acid 6	35

LIST OF SCHEMES

Scheme 1.	Synthesis of pentafluorobenzenesulfonamide 2	16
Scheme 2.	Synthesis of 4-mercaptopropanoictetrafluoro sulfonamide 4	17
Scheme 3.	Synthesis of CA IX targeting small molecule ligand 6	18
Scheme 4.	Synthesis of CA IX targeted Rhodamine B fluorescent probe 12	19
Scheme 5.	Synthesis of CA IX targeted Rhodamine B fluorescent probe 15	21
Scheme 6.	Synthesis of CA IX targeted fluorescent and radioimaging probe 22	22
Scheme 7.	Synthesis of 3-(2-pyridyldithio)propionate 26	23
Scheme 8.	Synthesis of functionalized self-immolative disulfide iron oxide nanoparticles 27	24

LIST OF TABLES

Table 1. Optimization table for synthesis of **4** **17**

Table 2. Optimization table for synthesis of **6** **18**

SYMBOLS/UNITS

λ	Wavelength
δ	Chemical shift
nm	Nanometer
$^{\circ}\text{C}$	Degree Celsius
mmol	Millimole
M	Molar
g	Gram
h	Hour
min	Minute
J	Coupling constant
nM	Nanomolar
mL	Milliliter
Hz/MHz	Hertz/Mega Hertz
R_f	Retention factor
ppm	Parts per million
H	Hydrogen
C	Carbon
F	Fluorine

ACRONYMS

TMS	Tetramethylsilane
NMR	Nuclear Magnetic Resonance
DCM	Dichloromethane
ACN	Acetonitrile
HRMS	High Resolution Mass Spectroscopy
CHCl ₃	Chloroform
CH ₃	Methyl
CDCl ₃	Chloroform-d
Et ₃ N	Triethylamine
THF	Tetrahydrofuran
DMF	<i>N,N</i> -Dimethyl formamide
APTES	3-Aminopropyltriethoxysilane
Na ₂ SO ₄	Sodium sulphate
OH	Hydroxyl
HATU	1-[Bis(dimethylamino)methylene]-1 <i>H</i> -1,2,3-triazolo[4,5- <i>b</i>]pyridinium 3-oxidhexafluorophosphate hexafluorophosphateazabenzotriazole tetramethyl uranium
PyBOP	Benzotriazol-1-yl-oxytripyrrolidinophosphonium hexafluorophosphate

DIPEA	<i>N, N'</i> -Diisopropylethylamine
TFA	Trifluoroacetic acid
TIS	Triisopropylsilane
EDT	1,2-Ethanedithiol
DCC	<i>N,N'</i> -Dicyclohexylcarbodiimide
MPA	Mercaptopropionic acid
NPs	Nanoparticles
CA	Carbonic anhydrase
DMSO	Dimethyl sulfoxide
PEG	Polyethylene glycol
SPION	Super Paramagnetic Iron oxide Nanoparticles
R.T.	Room Temperature
R.B	Round Bottom
s	Singlet
d	Doublet
dd	Doublet of doublet
t	Triplet
m	Multiplet

Chapter 1

Introduction

1.1. General Introduction

Oligodendrogliomas are a type of glioma that is believed to have originated from glial precursor cells or oligodendrocytes of the brain. Oligodendrogliomas account for 5–18% and in some cases even 25–33% of all intracranial gliomas.^{1–3} Oligodendrogliomas are known to affect mainly adults in the frontal and temporal lobe of the cerebellum.^{1–2} In different cellular compartments, antioxidant enzymes (AOEs) like superoxide dismutases (SODs), glutathione associated enzymes, peroxiredoxins, catalases and thioredoxin–thioredoxin reductase systems are situated. Majority of oligodendrogliomas express AOEs, especially thioredoxin reductase (TrxR) and manganese superoxide dismutase (MnSOD).⁴ Increased TrxR was associated with aggressive tumours and carbonic anhydrase IX enzyme (CA IX) was found to be expressed more often in MnSOD-positive tumors.⁵

Carbonic anhydrases (CA) are zinc-containing metalloenzymes known to catalyze reversible hydration of carbon dioxide.⁶ There are 12 catalytic isoforms of human CA, out of which CA IX is particularly important as it is rarely found in normal healthy tissues, but is expressed abundantly in several tumors, such as bladder, colorectal, lung, breast, and cervical carcinomas.^{7–9} CA IX is upregulated under hypoxic condition. The enzyme is transcriptionally activated through the HIF-1 transcription factor and builds up in malignant cells.⁵ Swiftly growing, inadequately organized and improperly proliferated cancer cells develop a deficiency of oxygen (usually less than 1% of total oxygen content) owing to the sudden change in their metabolism.¹⁰ This change in metabolic activity along with the rapid multiplication of

cells decreases the external pH of the cells making the microenvironment of these carcinogenic cells acidic owing to build-up of lactic acid.¹⁰⁻¹¹ The phenomenon competes with the formation of normal cells, and stimulates the growth of malignant cells. Thus, CA IX has proven to be a potent biomarker in oligodendroglial brain tumors.⁵ Thus it can be considered as a promising therapeutic target for brain tumours.

Our group has been working on various techniques on targeted drug delivery for detection and treatment of varied cancers¹²⁻¹⁵ as well as inflammatory diseases¹⁶⁻¹⁸ by utilizing small molecule targeting ligands. Several of these methods have been patented by the US and are currently in different stages of preclinical and clinical trials.¹⁹⁻²¹

Iron oxide nanoparticles can be inductively heated in the presence of a magnetic field. Hence, they are referred to as Super Paramagnetic Iron Oxide Nanoparticles (SPION). The cytotoxic effect of SPIONs due to hyperthermia induced by external magnetic field on solid tumors has been studied.²² Results from experimental studies indicate that hyperthermia is both an ideal complement to, as well as a strong sensitizer of radio and cytotoxic therapies.²³

1.2. Aim of the project

The aim of this project is to prepare a fluorescent imaging agent as well as a radioimaging tool for the detection of oligodendrogliomas over-expressing CA IX receptor and then develop a subsequent CA IX targeted theragnostic tool conjugated with iron oxide (Fe_3O_4) nanoparticles²⁴ followed by delivery to the active site of CA IX enzyme which is overexpressed in oligodendrogliomas for treatment using the principle of hyperthermia. The proposed bioconjugate comprises four parts i) a

CA IX targeted small molecule ligand ii) a hydrophilic spacer to increase the hydrophilicity of the conjugate as well as not decrease the specific binding affinity of the targeting ligand to the protein by increasing the distance between the small molecule ligand and the bioconjugate iii) fluorescent as well as a radioimaging agents that can acts as a diagnostic tool for early detection of oligodendrogliomas and iv) functionalized releasable nanoparticles that can act as therapeutic aid for hyperthermia strategy.

Chapter 2

Literature

Malignant cell environment is vastly different than normal cells, which is a key aspect for targeted therapy. Tumor growth comprises multifaceted interactions between the cells and their exclusive microenvironment which are characterized by acidic conditions and low pH.²⁵ The hypoxia-inducible enzyme CA IX which is one of the twelve isoforms of CA has been discussed as a biomarker and a potent therapeutic target in malignant gliomas.²⁶ The major class of CA inhibitors is aromatic and heterocyclic compounds possessing a primary sulfonamide group.²⁷ Benzene sulfonamides are the most abundantly available CA ligands. The aryl sulfonamide group interacts with zinc centre at the active site of CA IX by electron donor acceptor interactions. It has been found that a neutral pH (7.4) is ideal for maximum binding affinity of the ligand. Non-substituted benzenesulfonamide has a pK_a of 10.1.²⁸ Therefore, fluorinated benzene sulfonamides were considered which lower the pK_a of the targeted ligand and increase lipophilicity.²⁹ Several research groups have worked on developing various derivatives of non-fluorinated and polyfluorinated benzenesulfonamides and analyzed their properties of inhibition with various isoforms of CA.³⁰⁻³¹ The human CA IX has a deeper hydrophobic pocket in its active site than the other isoforms. Hence, introduction of a bulky cyclooctyl or cyclododecyl groups to the targeting ligand enhances affinity and selectivity towards CA IX.³⁰

The first report of using a bivalent disulfide-linked CA IX small molecule ligand with the payload containing a very effective cytotoxic maytansinoid DM1 as to treat CA IX positive renal cell carcinoma has been reported by Krall *et.al*. The study showed complete tumor regression in a xenograft mouse model.³¹⁻³² Additionally, a CA IX targeted small molecule tubulysin B drug conjugate for treatment of tumors expressing CA IX has been developed by , Low *et al.*³³ As CA IX is a cell surface antigen, there

has also been a report of CA IX-directed antibody conjugated immunoliposomes for targeted delivery of docetaxel to treat human lung cancer.³⁴ In another study, Cazzamalli *et al.* have designed four small molecule drug conjugates in which CA ligand, acetazolamide moiety, was coupled to an anticancer drug, monomethyl auristatin E, using a cleavable linker via different dipeptide aminoacid residues.³⁵ Low *et al.* have designed and delivered several bivalent small molecule drug conjugates to tumors overexpressing CA IX receptors for scintigraphy using a ^{99m}Tc-binding moiety and therapy using cytotoxic tubulysin B drug through a hydrophilic PEG linker. The cytotoxic conjugate suppressed tumour growth in a mouse model with HT-29 xenografts.³⁶ Other drug delivery strategies have also been explored involving surface modification of gold and silica nanoparticles by mounting CA ligands thus making them specific towards CA IX.³⁷⁻³⁹

Experimental Section

3.1. Materials and methods

All solvents or reagents used were supplied by Sigma Aldrich , Merck, Fisher chemicals and TCI Chemicals. H-Cys(Trt)-2-chlorotrityl resin and 1,2-Diaminoethane trityl resin was supplied by Iris biotech. Every reaction was done in clean, dry glassware with magnetic stirring. Thin layer chromatography was used to monitor reactions with the help of silica gel 60 F254 TLC glass plates provided by Merck. Glass syringes were used to transfer moisture and air sensitive reagents. Ethanol was distilled using Mg turnings under nitrogen atmosphere. Rotary Evaporator was used to evaporate volatile solvents under reduced pressure 40 °C. ¹H, ¹⁹F and ¹³C NMR spectra were recorded using Bruker AV 400MHz NMR spectrometer with TMS as an internal reference. The NMR solvents used were DMSO-*d*₆ and CDCl₃. The chemical shifts have been reported in delta (δ) units and expressed in ppm downfield from TMS. Mass spectra was recorded on a Bruker micro TOF-Q II spectrometer in positive mode electrospray ionization methods. The small molecule targeting ligand was purified using Büchi reveleris prep instrument with RP-PFP column (XSelect CSH Prep Fluorophenyl 5 μ m OBD) at a flow rate of 10 mL min⁻¹ with solvent A and B (A = MilliQ water with 0.1% TFA, B = ACN with 0.1% TFA)

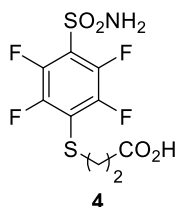
3.2. Synthesis of pentafluorobenzenesulfonamide (2)



Pentafluorobenzenesulfonyl chloride (1.00 g, 4.00 mmol) was dissolved using anhydrous THF (120 mL) in a 250 mL R,B flask at $-10\text{ }^{\circ}\text{C}$ followed by dropwise addition of 30% aq. ammonia (2.40 mL, 32.00 mmol) under constant stirring.

Monitoring of the reaction progress was done using TLC. On completion of 40 mins, reduced pressure was used to evaporate the solvent. The purification of crude product was done using column chromatography with a silica gel column (230–400 mesh) using 2:3 solution of 15:8.5 ethyl acetate in hexane to obtain pentafluorobenzenesulfonamide **2** (0.78 g, 84%) as a white coloured solid. m.p. $154\text{--}156\text{ }^{\circ}\text{C}$. TLC: $R_f = 0.5$ (2.5:7.5 EtOAc/hexane). IR: 3664, 3350 (N–H), 1492 (C=C), 1355 (S=O) cm^{-1} . ^1H NMR (400 MHz, DMSO- d_6): δ 8.46 (s, 2H). ^{13}C NMR (100 MHz, DMSO- d_6): δ 145.0 (d, ($^{19}\text{F}\text{-}^{13}\text{C}$) $J = 49.15$ Hz), 142.4 (d, ($^{19}\text{F}\text{-}^{13}\text{C}$) $J = 56.49$ Hz), 139.1 (t, ($^{19}\text{F}\text{-}^{13}\text{C}$) $J = 34.48$ Hz), 119.3 (t, ($^{19}\text{F}\text{-}^{13}\text{C}$) $J = 34.48$ Hz) ppm. ^{19}F NMR (400 MHz, DMSO- d_6): δ -139.0 (d, $J = 21.90$ Hz, 2F), -148.9 (t, $J = 44.80$ Hz, 1F), -160.5 (t, $J = 42.23$ Hz, 2F). MS (ESI) m/z $[\text{M}+\text{H}]^+$ calcd. for $\text{C}_6\text{H}_2\text{F}_5\text{NO}_2\text{S}$ calculated 247.9811, found 247.014.

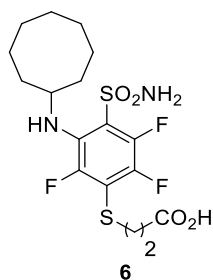
3.3. Synthesis of 3-((2,3,5,6-tetrafluoro-4-sulfamoylphenyl)thio)propanoic acid (4)



Pentafluorobenzenesulphonamide **2** (0.50 g, 2 mmol) was dissolved in 1 mL DMSO in a 5 mL R.B flask and constantly stirred at R.T. 3-Mercaptopropanoic acid **3** (0.19 mL, 2.2 mmol) and triethylamine as base (0.28 mL, 2.02 mmol) was subsequently added to the reaction mixture at R.T. The R.B containing reaction mixture was then heated at $70\text{ }^{\circ}\text{C}$ for 16 h. The reaction progress was monitored using TLC. Monitoring of the reaction progress was done using TLC. 20 mL of H_2O was added to the reaction mixture and 10 mL of EtOAc was used thrice to extract the crude product. It was dried using Na_2SO_4 . The purification of crude product was done

using column chromatography with a silica gel column (230–400 mesh) using 2:3 solution of ethyl acetate in hexane to get **4** (0.50 g, 75%) as light yellow solid. m.p. 168–169 °C. TLC: $R_f = 0.35$ (1:1 EtOAc/hexane). IR: 3406 (–NH₂), 3254 (–OH), 1701 (C=O), 1468 (C=C), 1364 (S=O) cm⁻¹. ¹H NMR (400 MHz, DMSO-*d*₆): δ 12.43 (s, 1H), 8.43 (s, 2H), 3.22 (t, $J = 13.55$ Hz, 2H), 2.60 (t, $J = 13.55$ Hz, 2H). ¹³C NMR (100 MHz, DMSO-*d*₆): δ 172.85, 145.84 (d, (¹⁹F-¹³C) $J = 19.81$ Hz), 141.70 (d, (¹⁹F-¹³C) $J = 20.54$ Hz), 123.22 (t, (¹⁹F-¹³C) $J = 30.81$ Hz), 118.61 (t, (¹⁹F-¹³C) $J = 41.81$ Hz), 35.14, 29.86, ppm. ¹⁹F NMR (100 MHz, DMSO-*d*₆): δ –139.18 (d, $J = 13.62$ Hz, 2F), –132.91 (d, $J = 13.62$ Hz, 2F) ppm. MS (ESI) m/z [M+Na]⁺ calcd. for C₉H₇F₄NO₄S₂ 355.9650, found 355.9700.

3.4. Synthesis of 3-((3-(cyclooctylamine)-2,5,6-trifluoro-4-sulfamoylphenyl)thio) propanoic acid (**6**)



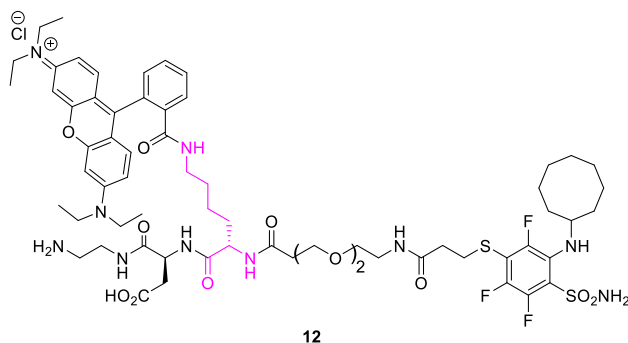
3-((2,3,5,6-tetrafluoro-4-sulfamoylphenyl)thio)

propanoic acid **3** (0.5 g, 1.50 mmol) was dissolved with 1 mL of DMSO in a 5 mL R.B flask under constant stirring at R.T. Triethylamine (0.41 mL, 3 mmol) followed by cyclooctylamine **5** (0.40 mL, 3 mmol) were added dropwise under constant stirring. The R.B

containing reaction mixture was then heated at 60 °C for 24 h. Monitoring of the reaction progress was done using TLC. 20 mL of H₂O was added to the reaction mixture and 10 mL of EtOAc was used thrice to extract the crude product. It was dried using Na₂SO₄. The purification of crude product was done using column chromatography with a silica gel column (230–400 mesh) using 2:3 solution of ethyl acetate in hexane to obtain ligand **6** (200 mg, 30%) as brown oily liquid. TLC: $R_f = 0.56$. IR: 3384 (–NH), 2929 (–OH), 1708 (C=O), 1460 (C=C), 1355 (S=O) cm⁻¹. ¹H NMR (400 MHz, DMSO-*d*₆): δ 12.48 (brs, 1H), 8.30 (s, 2H), 6.51 (brs, 1H), 3.32 (t, $J = 13.30$ Hz, 2H), 2.71–2.65 (m, 2H), 1.99 (t, $J = 21.58$ Hz,

2H), 1.82–1.66 (m, 12H) ppm. ^{13}C NMR (100 MHz, $\text{DMSO-}d_6$): δ 172.83, 146.14 (d, ($^{19}\text{F-}^{13}\text{C}$) $J = 16.14$ Hz), 143.10 (ddd, ($^{19}\text{F-}^{13}\text{C}$) $^1J = 4.68$ Hz, $^2J = 19.81$ Hz, $^3J = 3.6$ Hz), 140.58 (dd, ($^{19}\text{F-}^{13}\text{C}$) $^1J = 19.81$ Hz, $^2J = 4.40$ Hz), 132.38 (d, ($^{19}\text{F-}^{13}\text{C}$) $J = 13.30$ Hz), 119.84 (dd, ($^{19}\text{F-}^{13}\text{C}$) $^1J = 16.87$ Hz, $^2J = 5.13$ Hz), 11.46 (t, ($^{19}\text{F-}^{13}\text{C}$) $J = 43.28$ Hz), 55.81 (d, $J = 11.00$ Hz), 35.04, 32.64, 2.38, 25.59, 23.44 ppm. ^{19}F NMR (400 MHz, $\text{DMSO-}d_6$): δ -120.55 (d, $J = 12.26$ Hz, 7.48 Hz, 1F), -13.16 (dd, $^1J = 12.26$ Hz, $^2J = 12.26$ Hz 1F), -144.06 (d, $J = 2.25$ Hz, 1F) ppm. MS (ESI) m/z $[\text{M}+\text{H}]^+$ calcd. for $\text{C}_{17}\text{H}_{23}\text{F}_3\text{N}_2\text{O}_4\text{S}_2$ 441.1130, found 441.1190.

3.5. Synthesis of CA IX targeted Rhodamine B fluorescent probe (12)



1,2-Diaminotriethyl resin (100 mg, 0.105g/mol) was swelled using 5 mL DCM for thirty minutes by constant passage of nitrogen through the resin beads

inside the 15 mL peptide vessel which had been connected to a 500 mL brukner flask. A vacuum pump was used for drainage of DCM after thirty minutes and the beads were swelled again using 5 mL DMF for thirty minutes by constant passage of nitrogen. A solution containing Fmoc-Asp(O^tBu)-OH (108.00 mg, 0.26 mmol), HATU (100.00 mg, 0.26 mmol) and the base DIPEA (0.18 mL, 1.05 mmol) was made in 1 mL DMF and were added dropwise inside the peptide vessel having the resin. This coupling reaction was allowed to continue for 6 h with constant bubbling of nitrogen gas followed by washing of the resin beads with 3 mL of DMF thrice and then with 3 mL of isopropanol thrice. Reduced pressure was used for five minutes to dry the beads. Kaiser test was performed to confirm complete coupling. The Kaiser test reagents are as follows:

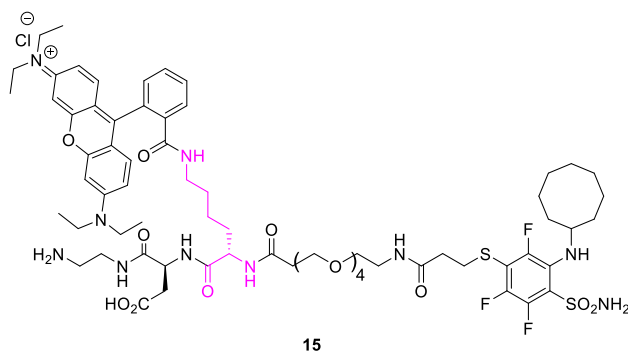
- i) A solution of 100 mg ninhydrin in 2 mL of ethanol
- ii) A solution of 80 g phenol in 20 mL ethanol

iii) A solution of 2 mL of a 0.001 M solution of KCN to 100 mL with pyridine

For deprotection of F-moc group a solution of 4 mL freshly prepared 20% piperidine in DMF was added inside the peptide vessel and nitrogen gas was bubbled through it for ten minutes. A vacuum pump was used to drain the reagent. The step for deprotection had to be repeated two times using 3 mL of the same deprotecting solution to guarantee complete deprotection of the Fmoc group. Next, 3 mL of DMF was used thrice as well as 3 mL of isopropanol was used thrice to wash the resin beads. Kaiser test was performed to confirm complete deprotection. Similarly, Fmoc-Lys(tfa)-OH (121.90 mg, 0.26 mmol), Fmoc-NH-PEG₂-COOH (104.90 mg, 0.26 mmol) and targeting ligand 6 (92.50 mg, 0.21 mmol) was coupled to the dipeptide. Lastly, the TFA-protected amine group of lysine was cleaved using a solution of 2M aqueous piperidine at R.T. for a duration of 12 h. Kaiser test. Was performed to confirm deprotection. Rhodamine B (125.80 mg, 0.26 mmol), HATU (100.00 mg, 0.26 mmol) and the base DIPEA (0.18 mL, 1.05 mmol) was dissolved in 1 mL DMF and were added dropwise inside the peptide vessel. This reaction was done at room temperature for 6 h. Kaiser test was used to confirm complete coupling. A cocktail solution containing TFA/H₂O/TIS having a ratio of (95:2.5:2.5) had been prepared freshly and 5 mL of the solution was added to the peptide vessel. Nitrogen gas was bubbled through it for forty minutes. A round bottom flask of 25 mL was used to collect the solution containing the bioconjugate. The same reaction for cleavage was done two more times by adding the cocktail solution of 2.5 mL for five minutes each for complete cleavage of bioconjugate from the resin beads. Reduced pressure was used to evaporate the cocktail solution. The gummy and concentrated compound was precipitated using 5 mL of icecold ether in a 15 mL centrifuge tube in an ice bath. The oily crude compound was washed using 3 mL of ice-cold ether for removing residual TFA and ethanedithiol. Reduced pressure was used to evaporate diethyl ether with rotatory

evaporator. MS (ESI) m/z $[M+H]^+$ calcd. for $C_{64}H_{89}F_3N_{10}O_{12}S_2$ 1310.6100, found 1311.7451.

3.6. Synthesis of CA IX targeted Rhodamine B fluorescent probe (15)

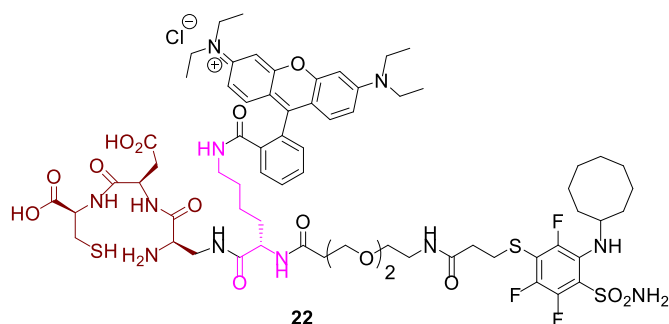


1,2-Diaminotriptyl resin (100 mg, 0.105g/mol) was swelled using 5 mL DCM for thirty minutes by constant passage of nitrogen through the resin beads

inside the 15 mL peptide vessel which had been connected to a 500 mL brukner flask. A vaccum pump was used for drainage of DCM after thirty minutes and the beads was swelled again using 5 mL DMF for thirty minutes by constant passage of nitrogen. A solution containing Fmoc-Asp(O'Bu)-OH (108.00 mg, 0.26 mmol), HATU (100.00 mg, 0.26 mmol) and the base DIPEA (0.18 mL, 1.05 mmol) was made in 1 mL DMF and were added dropwise inside the peptide vessel having the resin. This coupling reaction was allowed to continue for 6 h with constant bubbling of nitrogen gas followed by washing of the resin beads with 3 mL of DMF thrice and then with 3 mL of isopropanol thrice. Reduced pressure was used for five minutes to dry the beads. Kaiser test was performed to confirm complete coupling. For deprotection of F-moc group a solution of 4 mL freshly prepared 20% piperidine in DMF was added inside the peptide vessel and nitrogen gas was bubbled through it for ten minutes. A vaccum pump was used to drain the reagent. The step for deprotection had to be repeated two times using 3 mL of the same deprotecting solution to guarantee complete deprotection of the Fmoc group. Next, 3 mL of DMF was used thrice as well as 3 mL of isopropanol was used thrice to wash the resin beads. Kaiser test was performed to confirm complete deprotection. Similarly, Fmoc-Lys(tfa)-OH (121.90 mg, 0.26 mmol), Fmoc-NH-PEG4-

COOH (139.50 mg, 0.26 mmol) and targeting ligand 6 (92.50 mg, 0.21 mmol) was coupled to the dipeptide. Lastly, the TFA-protected amine group of lysine was cleaved using a solution of 2M aqueous piperidine at R.T. for a duration of 12 h. Kaiser test. Was performed to confirm deprotection. Rhodamine B (125.80 mg, 0.26 mmol), HATU (100.00 mg, 0.26 mmol) and the base DIPEA (0.18 mL, 1.05 mmol) was dissolved in 1 mL DMF and were added dropwise inside the peptide vessel. This reaction was done at room temperature for 6 h. Kaiser test was used to confirm complete coupling. A cocktail solution containing TFA/H₂O/TIS having a ratio of (95:2.5:2.5) had been prepared freshly and 5 mL of the solution was added to the peptide vessel. Nitrogen gas was bubbled through it for forty minutes. A round bottom flask of 25 mL was used to collect the solution containing the bioconjugate. The same reaction for cleavage was done two more times by adding the cocktail solution of 2.5 mL for five minutes each for complete cleavage of bioconjugate from the resin beads. Reduced pressure was used to evaporate the cocktail solution. The gummy and concentrated compound was precipitated using 5 mL of ice cold ether in a 15 mL centrifuge tube in an ice bath. The oily crude compound was washed using 3 mL of ice-cold ether for removing residual TFA and ethanedithiol. Reduced pressure was used to evaporate diethyl ether with rotatory evaporator.

3.7. Synthesis of CA IX targeted fluorescent and radioimaging probe (22).



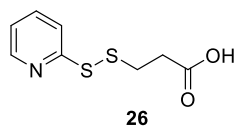
H-Cys(Trt)-2-chlorotrityl resin (100 mg, 0.64 g/mol) was swelled using 5 mL DCM for thirty minutes by

constant passage of nitrogen through the resin beads inside the 15 mL

peptide vessel which had been connected to a 500 mL brukner flask. A vaccum pump was used for drainage of DCM after thirty minutes and the beads was swelled again using 5 mL DMF for thirty minutes by constant passage of nitrogen. A solution containing Fmoc-Asp(O^tBu)-OH (97.20 mg, 0.23 mmol), HATU (90.00 mg, 0.23 mmol) and the base DIPEA (0.16 mL, 0.94 mmol) was made in 1 mL DMF and were added dropwise inside the peptide vessel having the resin. This coupling reaction was allowed to continue for 6 h with constant bubbling of nitrogen gas followed by washing of the resin beads with 3 mL of DMF thrice and then with 3 mL of isopropanol thrice. Reduced pressure was used for five minutes to dry the beads. Kaiser test was performed to confirm complete coupling. For deprotection of F-moc group a solution of 4 mL freshly prepared 20% piperidine in DMF was added inside the peptide vessel and nitrogen gas was bubbled through it for ten minutes. A vaccum pump was used to drain the reagent. The step for deprotection had to be repeated two times using 3 mL of the same deprotecting solution to guarantee complete deprotection of the Fmoc group. Next, 3 mL of DMF was used thrice as well as 3 mL of isopropanol was used thrice to wash the resin beads. Kaiser test was performed to confirm complete deprotection. A solution containing Boc-Dap(Fmoc)-OH (100.80 mg, 0.23 mmol), HATU (100.00 mg, 0.26 mmol) and the base DIPEA (0.18 mL, 1.05 mmol) was made in 1 mL DMF and were added dropwise inside the peptide vessel having the resin using Pasteur pipette and nitrogen gas was constantly bubbled for 6 h. , 3 mL of DMF was used thrice as well as 3 mL of isopropanol was used thrice to wash the resin beads. Kaiser test was used to confirm complete coupling. Reduced pressure was used to dry the resin beads for 5 min. Similarly, Fmoc-Lys(tfa)-OH (109.0 mg, 0.23 mmol), Fmoc-NH-PEG₂-COOH (75.50 mg, 0.18 mmol) and targeting ligand 6 (83.2 mg, 0.21 mmol) was coupled to the tripeptide. Lastly, the TFA-protected amine group of lysine was cleaved using a solution of 2M aqueous piperidine at R.T. for a duration of 12 h. Kaiser test. Was performed to

confirm deprotection. Rhodamine B (125.80 mg, 0.26 mmol), HATU (90.00 mg, 0.23 mmol) and the base DIPEA (0.16 mL, 0.94 mmol) was dissolved in 1 mL DMF and were added dropwise inside the peptide vessel. This reaction was done at room temperature for 6 h. Kaiser test was used to confirm complete coupling. A cocktail solution containing TFA/EDT/TIS/H₂O having a ratio of (92.5:2.5:2.5:2.5) had been prepared freshly and 5 mL of the solution was added to the peptide vessel. Nitrogen gas was bubbled through it for forty minutes. A round bottom flask of 25 mL was used to collect the solution containing the bioconjugate. The same reaction for cleavage was done two more times by adding the cocktail solution of 2.5 mL for five minutes each for complete cleavage of bioconjugate from the resin beads. Reduced pressure was used to evaporate the cocktail solution. The gummy and concentrated compound was precipitated using 5 mL of ice cold ether in a 15 mL centrifuge tube in an ice bath. The oily crude compound was washed using 3 mL of ice-cold ether for removing residual TFA and ethanedithiol. Reduced pressure was used to evaporate diethyl ether with rotatory evaporator.

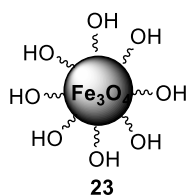
3.8. Synthesis of 3-(2-pyridinyldithio)propanoic acid (26)



2-Aldrithiol (0.5 g, 2.27 mmol) was dissolved using 10 mL of dry ethanol in a 25 mL R.B flask under constant stirring at R.T. 3-mercaptopropanoic acid (0.40 mL, 4.52 mmol) was dissolved in 2 mL anhydrous ethanol and added dropwise to the reaction mixture under stirring condition following the addition of acetic acid (50 μ L, 3.48 mmol). The reaction was allowed to continue for 24 h. TLC was used for monitoring reaction progress. After completion, reduced pressure was used to evaporate ethanol to give yellowish solid. It was dried using vaccum pump for two hours to remove acetic acid traces. Purification of the crude product was done using column chromatography with neutral alumina column using a 2:3 mixture of ethyl acetate in hexane to elute 3-(2-pyridinyldithio)propanoic acid **26**

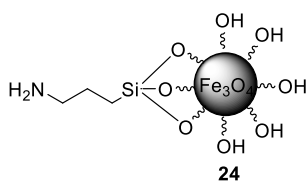
in 60% yield as a yellow solid. ^1H NMR (400 MHz, CDCl_3): δ 14.04 (s, 1H), 7.55–7.49 (m, 4H), 7.34 (t, $J = 15.56$, 2H), 6.73 (t, $J = 12.80$, 2H) ppm. ^{13}C NMR (100 MHz, CDCl_3): δ 176.68, 138.01, 136.88, 133.83, 114.10, 60.42, 29.67 ppm.

3.9. Synthesis of Iron oxide nanoparticles (23)



Ferric chloride hexahydrate (232 mg, 1.44 mmol) and ferrous sulfate heptahydrate (200 mg, 0.72 mmol) were dissolved in 20 mL of deoxygenated water and sonicated for thirty minutes. This mixture was then added dropwise to a 2M solution of NaOH under constant stirring. The reaction mixture was then refluxed for 8 h at 80 °C. It was then cooled to R.T. and the dark brown magnetic precipitate was washed with 10 mL of distilled water for five times and then with 10 mL of ethanol twice following decantation in the presence of a magnet. The nanoparticles were dried on a petri dish.

3.10. Synthesis of APTES (3-aminopropyltriethoxysilane) functionalized iron oxide nanoparticles



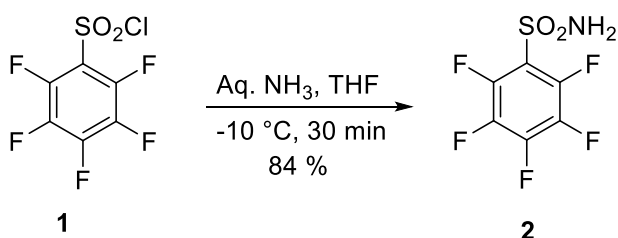
The SPIONs (300 mg) were suspended in dry ethanol (100 mL) in a 250 mL R.B. flask with vigorous stirring at R.T. for 20 min under nitrogen atmosphere and sonicated for one hour with the help of a sonicator. To the SPION suspension, 3-Aminopropyltriethoxysilane was added in a dropwise manner at R.T. under constant stirring under nitrogen atmosphere. It was allowed to reflux for 24 h under nitrogen atmosphere and constant stirring. After completion of the reaction ethanol was decanted after cooling the reaction mixture to R.T. The functionalised nanoparticles were then washed using 5 mL of ethanol for five times and filtered using decantation in the presence of a magnet. The precipitate of Fe_2O_3 nanoparticles functionalised with APTES **24** was dried in the oven for 24 h at 50 °C.

Chapter 4

Results and Discussion

4.1 Synthesis of small molecule ligand targeting CA IX

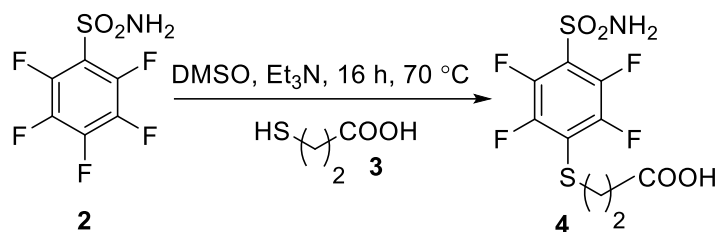
The CA IX targeted ligand was synthesized in three steps starting with pentafluorobenzenesulfonyl chloride **1**. **1** undergoes a S_N2 substitution with aqueous ammonia to give pentafluorobenzenesulfonamide **2** in good yield 84% (Scheme 1).



Scheme 1. Synthesis of pentafluorobenzenesulfonamide **2**

Pentafluorobenzenesulfonamide **2** undergoes addition elimination reaction at the para position to form para-substituted benzenesulfonamide. In the reaction, **2** was dissolved in DMSO and reacted with mercaptopropionic acid **3** (1.1 equiv.) acting as the nucleophile, Et₃N (1.0 equiv.) acting as the base as given in the optimization table below. In **2**, the most probable position for attack by nucleophile mercaptopropionic acid is *para* because the sulfonamide group is ortho para directing but due to the presence of steric effect at ortho position, the substitution occurs at the para position giving 75% yield of **4**. The optimization table gives the effects of solvent polarity, number of equivalents of nucleophile and base as well as temperature on the percentage yield of **4**. The increase in the equivalents number of the nucleophile **3** and time of reaction (entries 1-3, Table 1) resulted in poor yield due formation of side products. By changing the solvent to a highly polar solvent DMSO, reducing reaction time, temperature and keeping the equivalent of base at 1.0 equiv. and

nucleophile at 1.1 equiv. the substitution reaction was easier with greater yield of **4** at 75% (entry 5, Table 1).



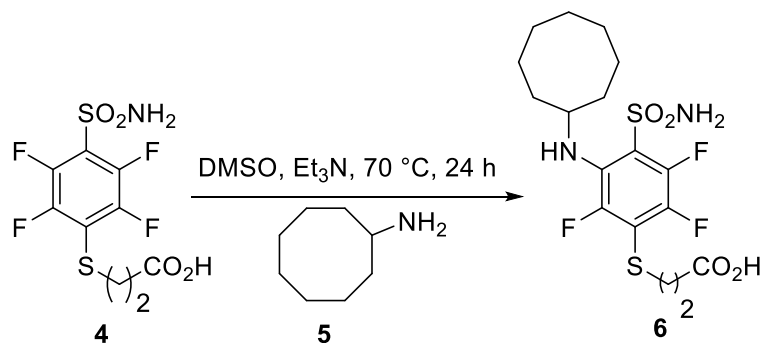
Scheme 2. Synthesis of 4-mercaptopropanoictetrafluorobenzene sulfonamide **4**

Entry	Reaction Conditions	% Yield 4
1.	3 (1.1 equiv.), Methanol, Et ₃ N (1.01 equiv.), 80 °C, 22 h	37
2.	3 (2.0 equiv.), DMSO, Et ₃ N (1.01 equiv.), 70 °C, 24 h	25
3.	3 (1.3 equiv.), DMSO, Et ₃ N (1.01 equiv.), 80 °C, 24 h	40
4.	3 (1.1 equiv.), DMSO, Et ₃ N (1.01 equiv.), 80 °C, 24 h	58
5.	3 (1.1 equiv.), DMSO, Et ₃ N (1.01 equiv.), 70 °C, 16 h	75

Table 1. Optimization table for the synthesis of **4**

4-mercaptopropionic-2,3,5,6-tetrafluorobenzene sulfonamide **4** undergoes another addition elimination reaction at the ortho position of the sulfonamide derivative. In this reaction, **4** was dissolved in DMSO and reacted with cyclooctyl amine **5** (2.0 equiv.) acting as the nucleophile, Et₃N (2.0 equiv.) acting as the base. **4** undergoes a nucleophilic substitution by cyclooctyl amine to produce small molecule targeting ligand **6** with very low yield of 30% (Scheme 3, Table 2). In **4**, the most probable nucleophilic attack site is the C2 carbon or the C6 carbon because comparatively they have more electron deficiency due to the presence of thiopropanoic acid at C4 as the sulphur atom is electron donating. The yield percentage of **6** was slightly increased by doubling the equivalents of both

nucleophile and base. The synthesized compound **6** may be utilized as a novel CA IX targeting small molecule ligand.



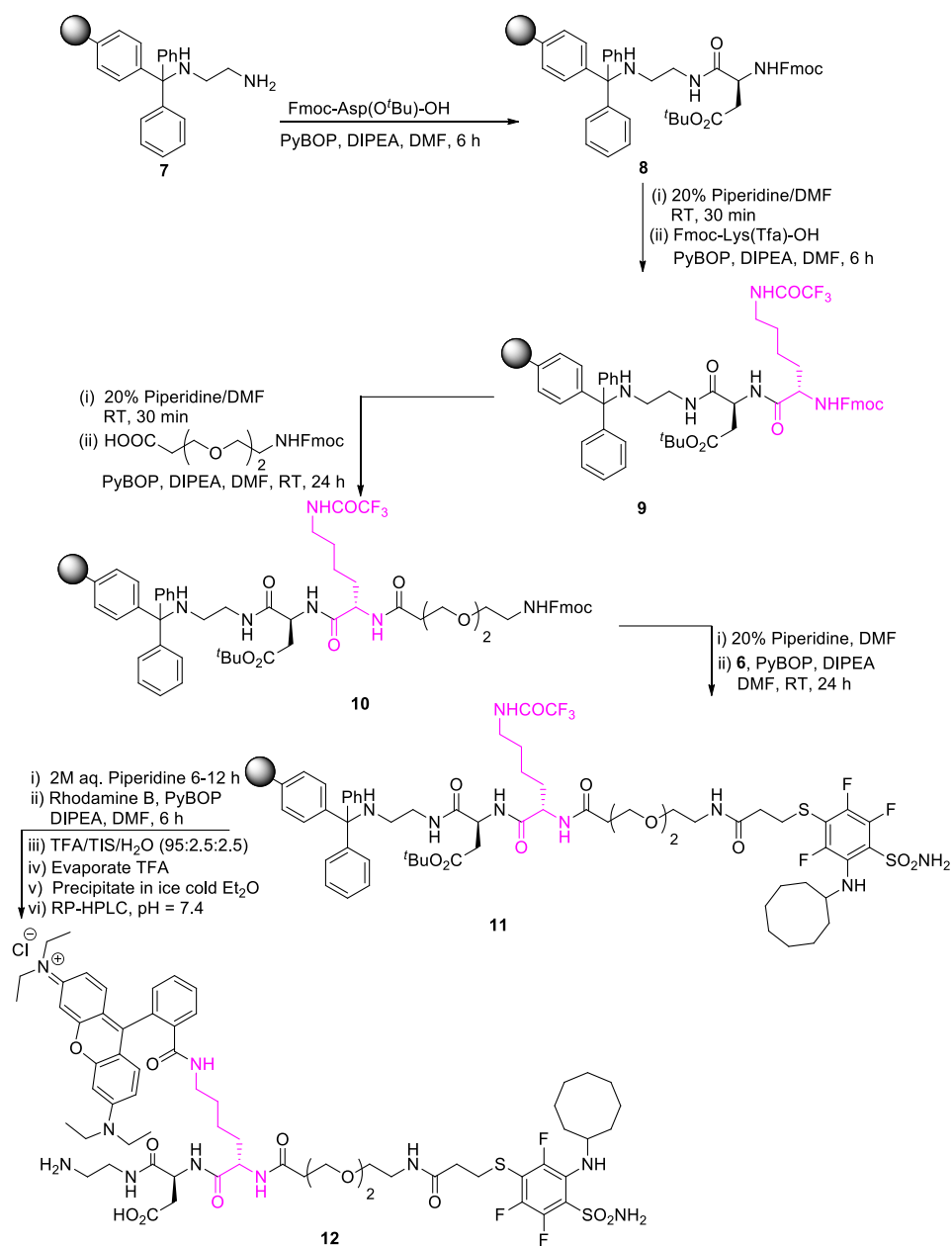
Scheme 3. Synthesis of CA IX targeting small molecule ligand **6**

Entry	Reaction conditions	% Yield 6
1.	5 (1.1 equiv.), DMSO, Et ₃ N (1.01 equiv.), 60 °C, 24 h	24
2.	5 (2.0 equiv.), DMSO, Et ₃ N (2.0 equiv.), 60 °C, 24 h	30

Table 2. Optimization table for synthesis of **6**

4.2. Synthesis of CA IX targeted Rhodamine B fluorescent probe **12**

The solid phase peptide synthesis (SPPS) to produce targeting ligand and hydrophilic linker conjugated fluorescent probe (Rhodamine B) **12** for detection of oligodendrogliomas was started using 1,2-diaminoethanetrityl resin. 1,2-diaminoethanetrityl resin **7** has a free NH₂ group which was coupled to the free COOH group of Fmoc-Asp-(O^tBu)-OH to give **8**. After deprotection of NHFmoc group from **8**, the Boc-Lys(Tfa)-OH was coupled to the free NH₂ group to form **9**. Subsequently, **9** was coupled to COOH group of



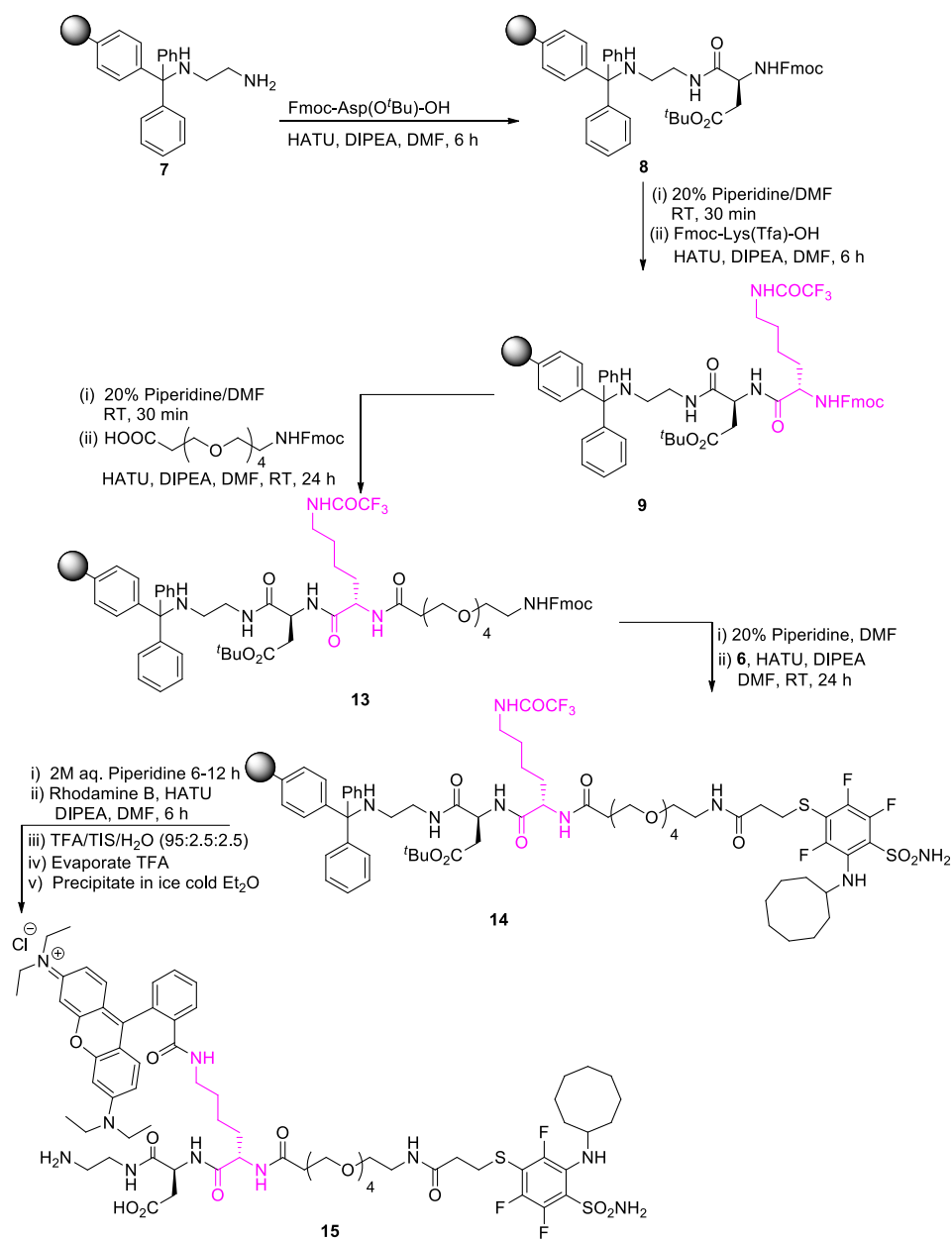
Scheme 4. Synthesis of CA IX targeted Rhodamine B fluorescent probe **12**

NHFmoc protected PEG linker to afford **10**. After deprotection of NHFmoc group from **8**, the small molecule ligand **6** was attached to the spacer to form **11**. TFA group present in the masked polypeptide chain **11** was deprotected using aqueous piperidine solution and then coupled with

Rhodamine B. The ligand conjugated hydrophilic spacer with Rhodamine B **12** was released from resin beads on treatment with a cocktail solution of TFA/H₂O/TIS in the ratio 95:2.5:2.5. Reduced pressure was used to concentrate the mother liquor obtained from resin cleavage using rotary evaporator. Ice-cold ether was added to the viscous solution in a dropwise manner to precipitate dark pink Rhodamine B conjugate **12**.

4.3. Synthesis of CA IX targeted Rhodamine B fluorescent probe 15

The solid phase peptide synthesis (SPPS) to produce targeting ligand and hydrophilic linker conjugated fluorescent probe (Rhodamine B) **15** for detection of oligodendrogliomas was started using 1,2-diaminoethanetriyl resin. 1,2-diaminoethanetriyl resin **7** has a free NH₂ group which was coupled to the free COOH group of Fmoc-Asp-(O^tBu)-OH to give **8**. After deprotection of NHFmoc group from **8**, the Boc-Lys(Tfa)-OH was coupled to the free NH₂ group to form tripeptide chain **9**. Subsequently, **9** was coupled with free carboxylic group of NHFmoc protected PEG₄ linker to afford **13**. After deprotection of NHFmoc group from **13**, the small molecule ligand **6** was attached to the PEG₄ linker to form **14**. The TFA group present in the masked polypeptide chain **14** was deprotected using 2 M aqueous piperidine solution and then coupled with Rhodamine B. The ligand conjugated hydrophilic spacer with Rhodamine B **15** was released from resin beads on treatment with a cocktail solution of TFA/H₂O/TIS in the ratio 95:2.5:2.5. Reduced pressure was used to concentrate the mother liquor obtained from resin cleavage using rotary evaporator. Ice-cold ether was added to the viscous solution in a dropwise manner to precipitate dark pink Rhodamine B conjugate **15**.

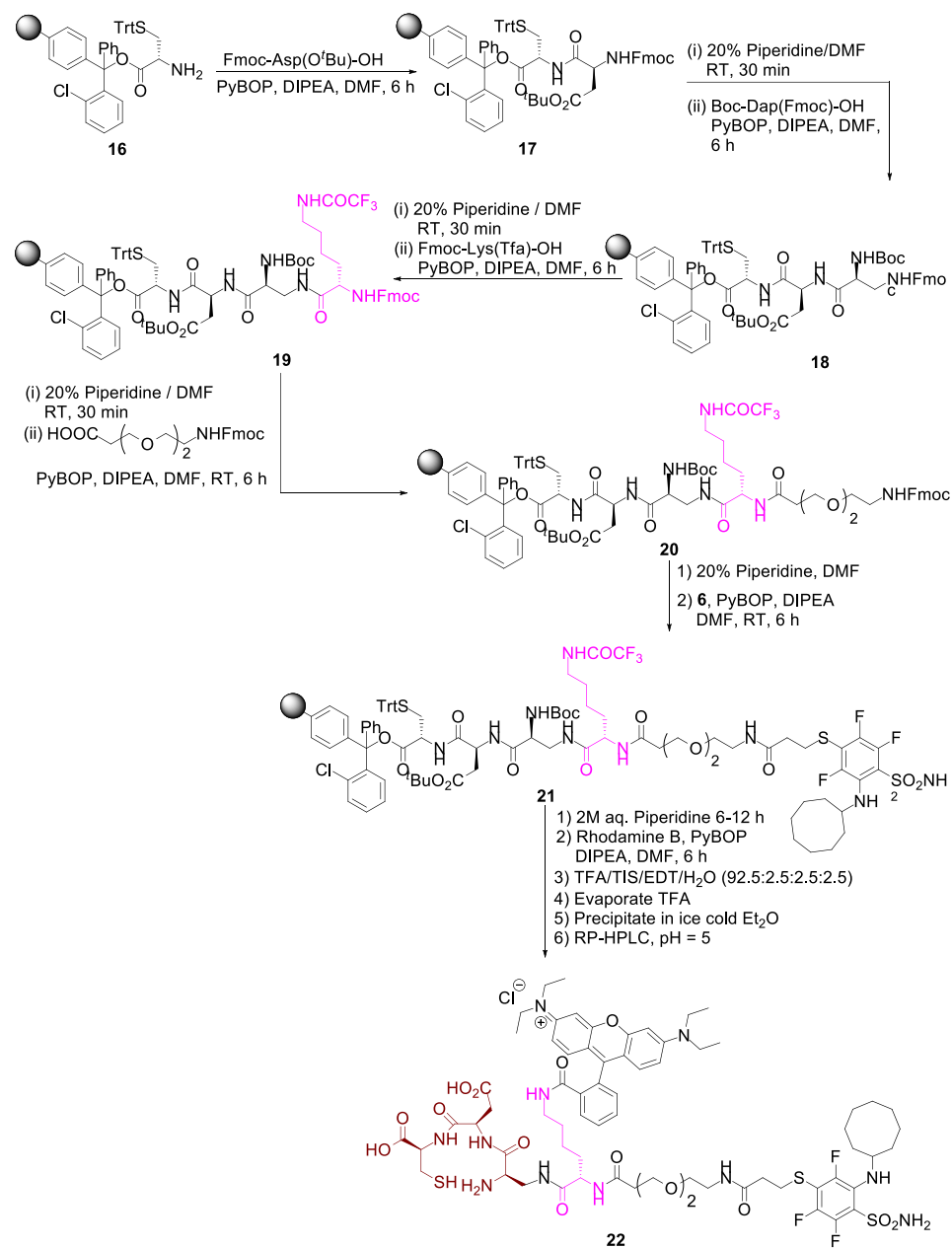


Scheme 5. Synthesis of CA IX targeted Rhodamine B fluorescent probe

15

4.4 Synthesis of CA IX targeted fluorescent and radioimaging probe **22**

The synthesis of hydrophilic spacer conjugated ligand was started with cysteine chlorotrityl resin **16** (Scheme 6). The free NH₂ group of the resin was coupled with free COOH group of

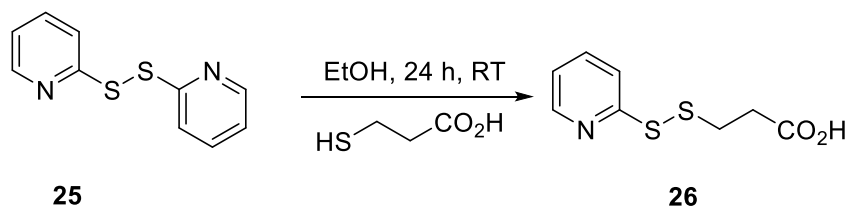


Scheme 6. Synthesis of CA IX targeted fluorescent and radioimaging probe **22**

Fmoc-Asp(O^tBu)-OH to give dipeptide chain **17**. After deprotection of NHFmoc group from **17**, the Boc-Dap(Fmoc)-OH was coupled with free NH₂ group to form tripeptide **18**. After deprotection of NHFmoc group from **18**, the Fmoc-Lys(Tfa)-OH was coupled with the free NH₂ group to form tetrapeptide linker **19**. Subsequently, **19** was coupled with free COOH group of NHFmoc protected PEG₂ linker to afford **20**. After deprotection of NHFmoc group from **20**, the small molecule ligand **6** were attached with the hydrophilic PEG linker by standard SPPS protocol to form **21**. After deprotection of the NHTfa group from **21**, Rhodamine B will be attached to NH₂ group of lysine moiety and the ligand targeted chelating linker Rhodamine B conjugate **22** was detached from resin beads on treatment with a cocktail solution containing TFA/EDT/TIS/H₂O in the ratio 92.5:2.5:2.5:2.5. Reduced pressure was used to concentrate the mother liquor obtained from resin cleavage using rotary evaporator. Ice-cold ether was added dropwise to the viscous solution to precipitate the dark pink rhodamine B conjugate **22**.

4.5. Synthesis of 3-(2-pyridinyldithio)propanoic acid **26**

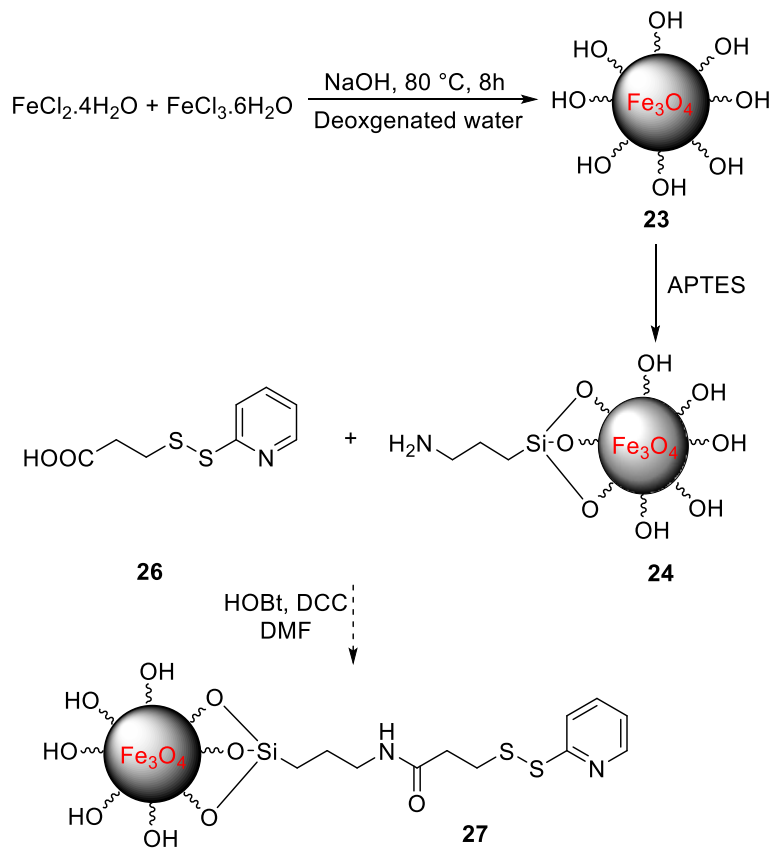
2-Aldrithiol was dissolved in dry Ethanol and then 3-Mercaptopropanoic acid was added to it by a thiol-disulfide exchange in presence of acetic acid to prevent dimerization of 3-Mercaptopropionic acid to produce 3-(2-pyridinyldithio)propanoic acid **26** in 60% yield (Scheme 8)



Scheme 7. Synthesis of 3-(2-pyridinyldithio)propanoic acid **26**

4.6 Synthesis of APTES functionalized self-releasable Fe₂O₃ nanoparticles **27**

SPIONs **23** were synthesized using co-precipitation methodology followed by functionalization with a silanizing agent, 3-Aminopropyltriethoxysilane (APTES) producing surface functionalized Fe₂O₃ nanoparticles **24**. Further, the amine group in **24** will have to be coupled to the acid group of 3-(2-pyridyldithio)propanoic acid **25** in order to give activated Fe₂O₃ nanoparticles via disulphide linkage **27** (Scheme 8).



Scheme 8. Synthesis of functionalized self-immolative disulfide ironoxide nanoparticles **27**

Chapter 5

Conclusion

In this particular research project, a new sulfonamide derivative (CA Inhibitor), a small molecule targeting ligand **6** was successfully synthesized in a three-step process with overall 19% yield. The Carbonic Anhydrase IX targeted small molecule ligand **6** was further conjugated with required hydrophilic PEG linker and fluorescent probe using solid phase peptide synthesis for synthesis of biconjugates **12** and **15**. The targeting ligand was also used to prepare a CA IX targeting fluorescent and radioimaging probe **22**.

For further application of detecting and treating oligodendrogliomas using functionalized releasable Fe₂O₃ nanoparticles by utilizing their property of hyperthermia. The synthesized radioimaging and fluorescent probe **22** has to be attached to Fe₂O₃ nanoparticles. The Fe₂O₃ nanoparticles can also be a therapeutic agent for targeting oligodendrogliomas that overexpress Carbonic Anhydrase IX receptor.

Furthermore, Fe₂O₃ nanoparticles **23** were prepared using co-precipitation method followed by functionalisation with salanizing agent APTES give Fe₂O₃ nanoparticles **24**.

The APTES functionalized Fe₂O₃ nanoparticles **24** will have to be transformed into disulfide activated Fe₂O₃ nanoparticles **27**. These activated Fe₂O₃ nanoparticles **27** will have to be coupled with the CA IX targeted bioconjugate **22** to finally produce selfreleasable Fe₂O₃ nanoparticles carrying Carbonic Anhydrase IX bioconjugate for detecting and treating oligodendrogliomas.

APPENDIX-A

^1H , ^{13}C , ^{19}F NMR

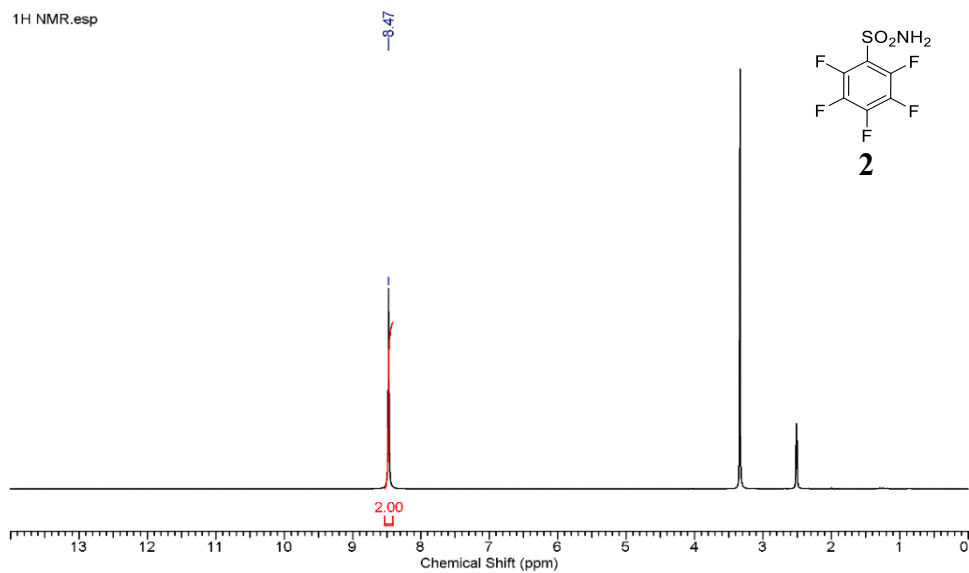


Figure 1: ^1H NMR spectrum of pentafluorobenzenesulphonamide **2** in $\text{DMSO-}d_6$

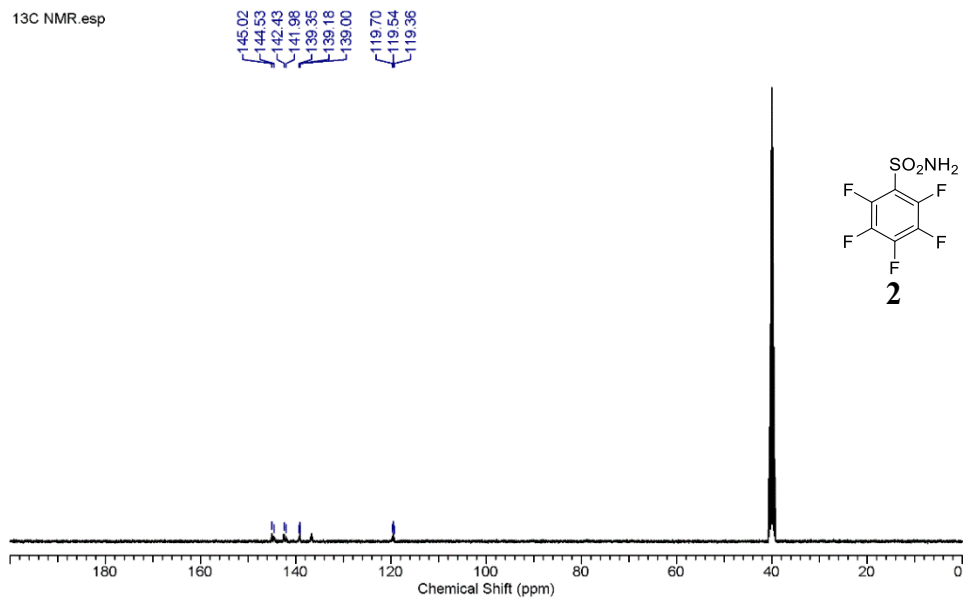


Figure 2: ^{13}C NMR spectrum of pentafluorobenzenesulphonamide **2** in $\text{DMSO-}d_6$

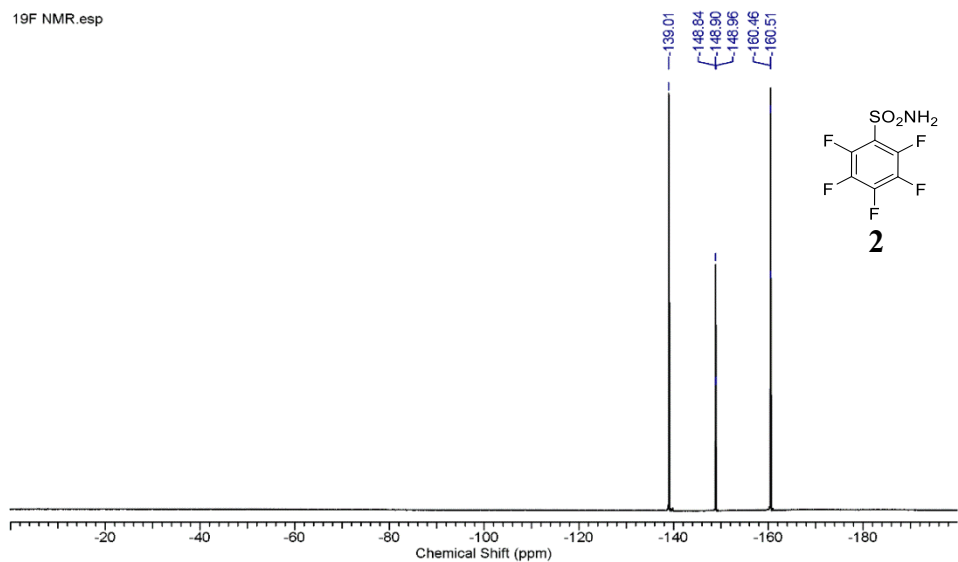


Figure 3: ^{19}F NMR spectrum of pentafluorobenzenesulphonamide **2** in $\text{DMSO-}d_6$

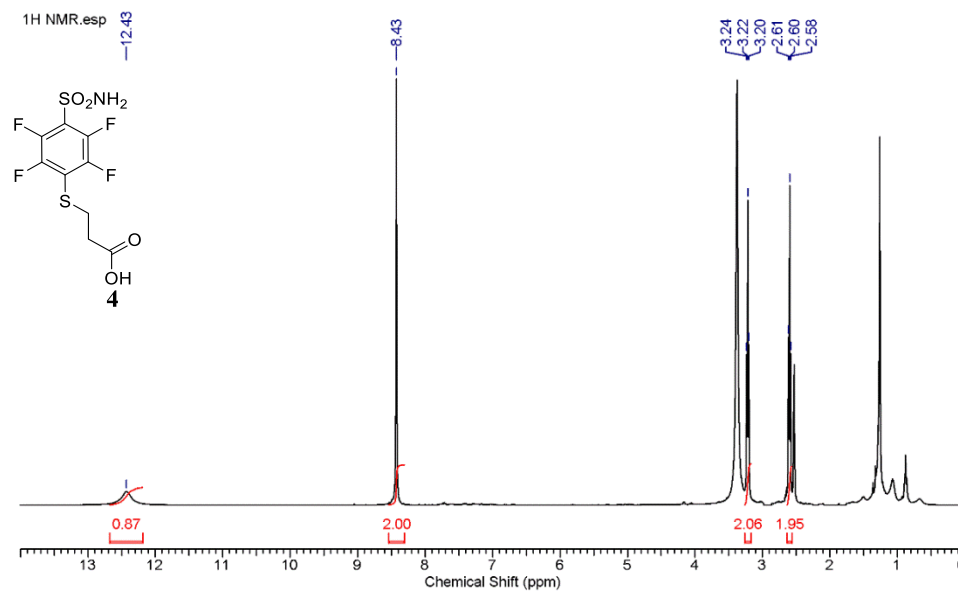


Figure 4: ^1H NMR spectrum of 3-((2,3,5,6-tetrafluoro-4-sulfamoyl phenyl)thio)propanoic acid **4** in $\text{DMSO-}d_6$

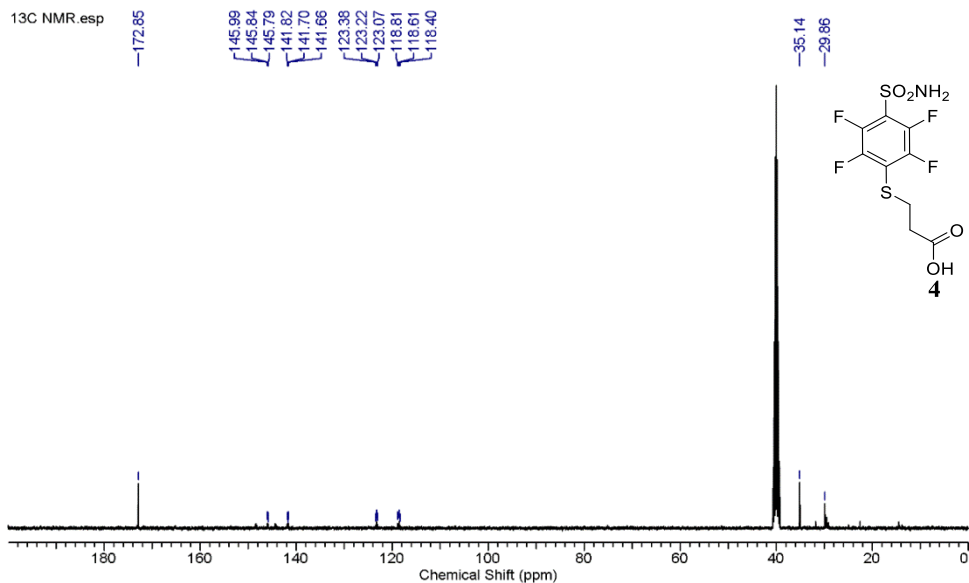


Figure 5: ^{13}C NMR spectrum of 3-((2,3,5,6-tetrafluoro-4-sulfamoyl phenyl)thio)propanoic acid **4** in $\text{DMSO-}d_6$

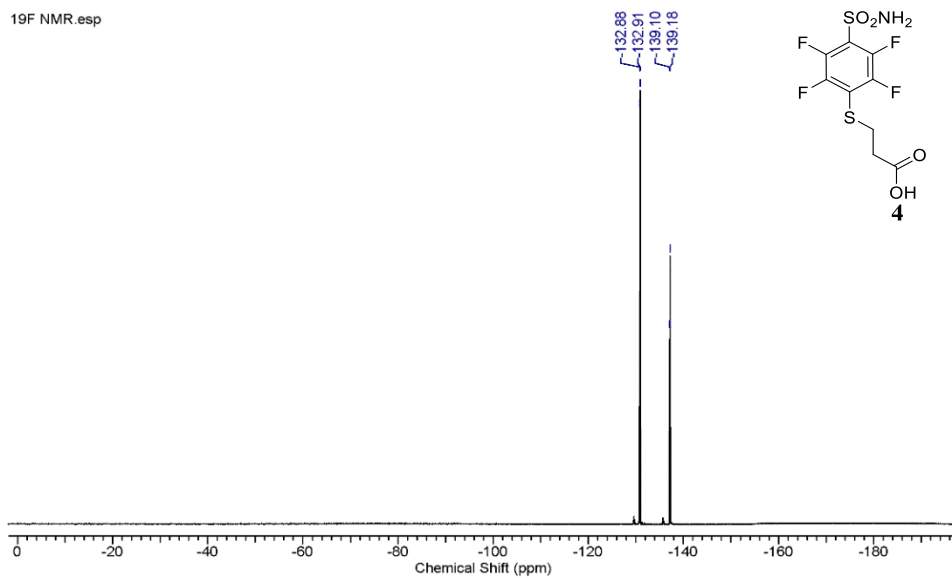


Figure 6: ^{19}F NMR spectrum of 3-((2,3,5,6-tetrafluoro-4-sulfamoyl phenyl)thio)propanoic acid **4** in $\text{DMSO-}d_6$

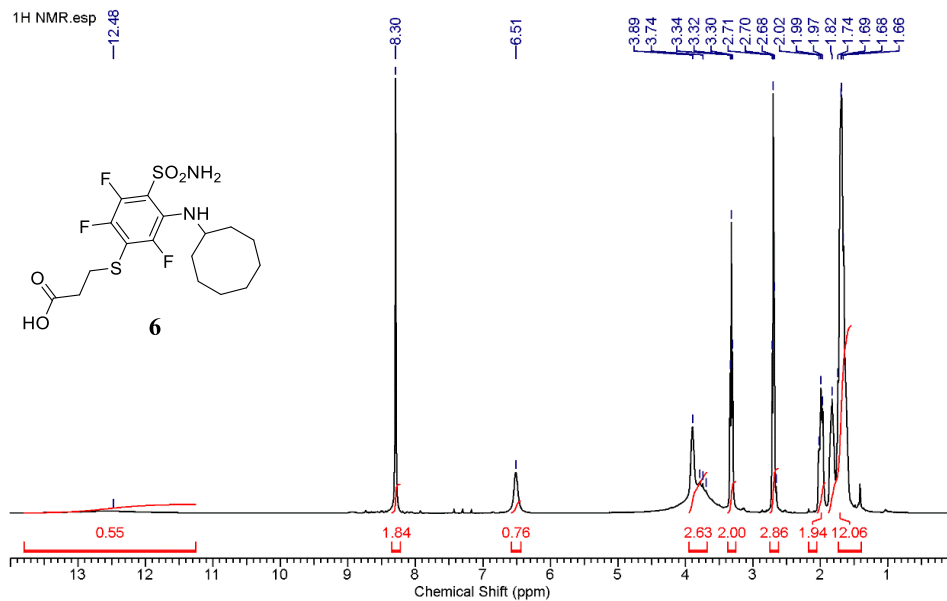


Figure 7: ^1H NMR spectrum of 3-((3-(cyclooctylamine)-2,5,6-trifluoro-4-sulfamoylphenyl)thio) propanoic acid **6** in $\text{DMSO-}d_6$

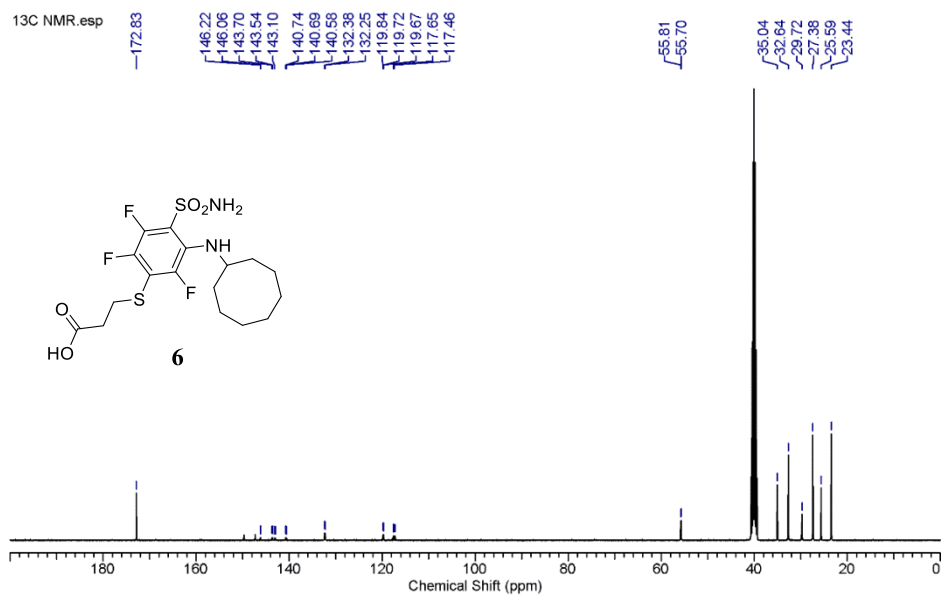


Figure 8: ^{13}C NMR spectrum of 3-((3-(cyclooctylamine)-2,5,6-trifluoro-4-sulfamoylphenyl)thio) propanoic acid **6** in $\text{DMSO-}d_6$

19F NMR 1.esp

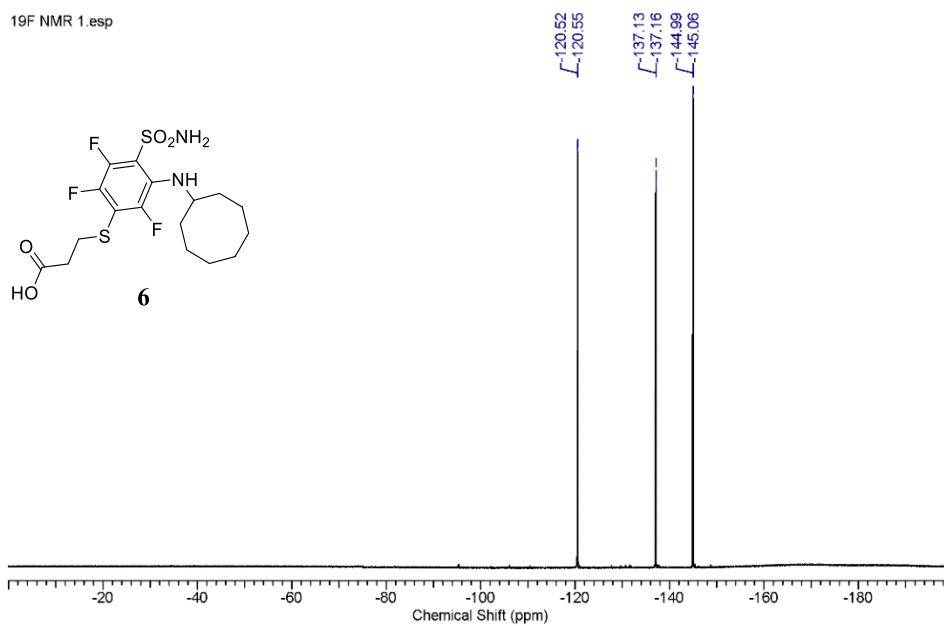


Figure 9: ¹⁹F NMR spectrum of 3-((3-(cyclooctylamine)-2,5,6-trifluoro-4-sulfamoylphenyl)thio) propanoic acid **6** in DMSO-*d*₆

1H NMR 1.esp

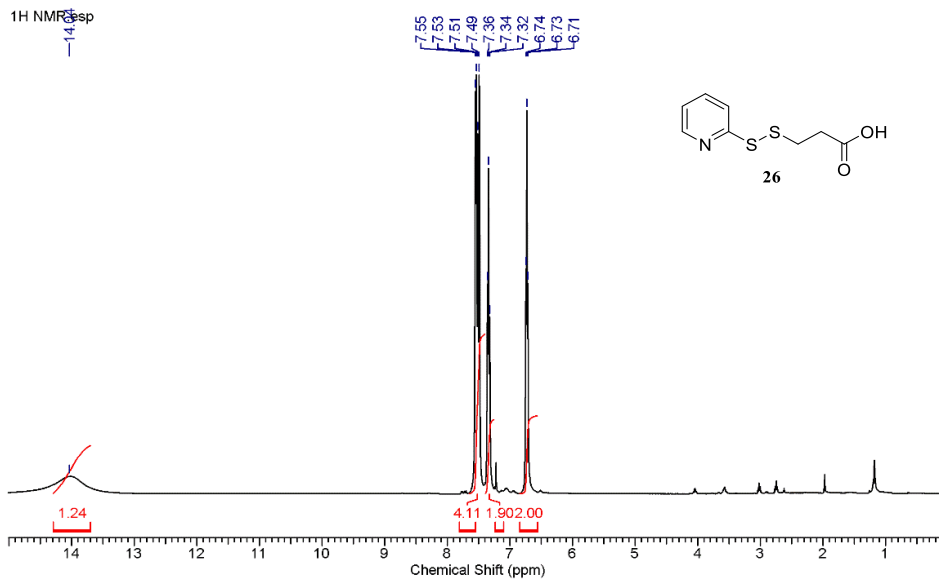


Figure 10: ¹H NMR spectrum of 3-(2-pyridinyldithio)propanoic acid **26** in CDCl₃

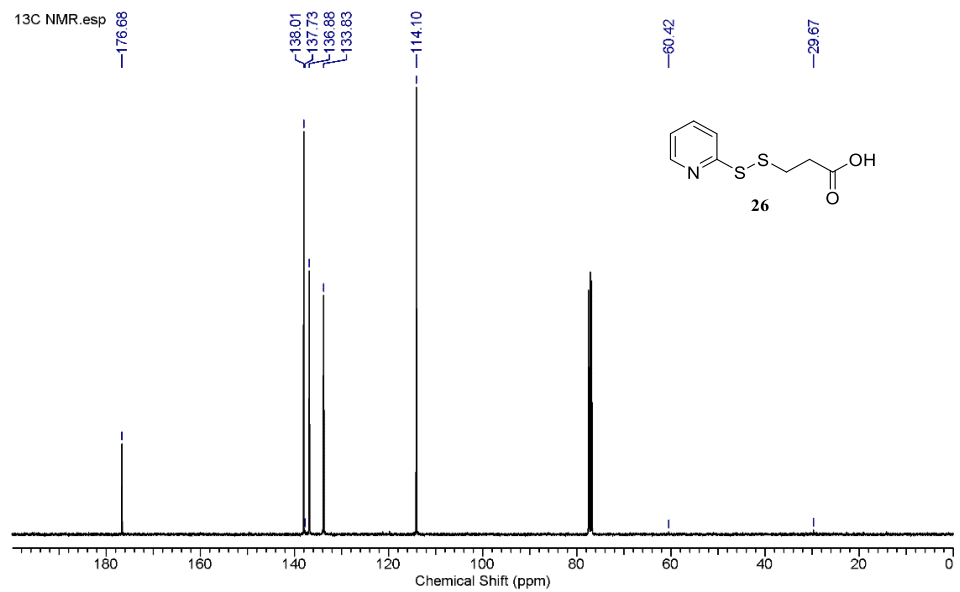


Figure 11: ^{13}C NMR spectrum of 3-(2-pyridinyldithio)propanoic acid **26** in CDCl_3

Mass Spectra

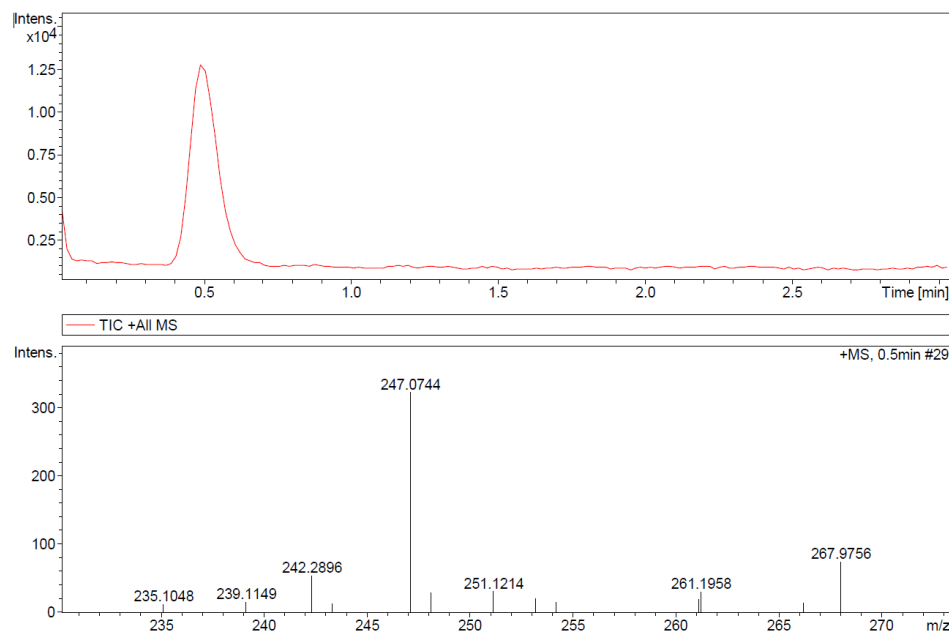


Figure 12: MS(ESI) of pentafluorobenzenesulfonamide **2**

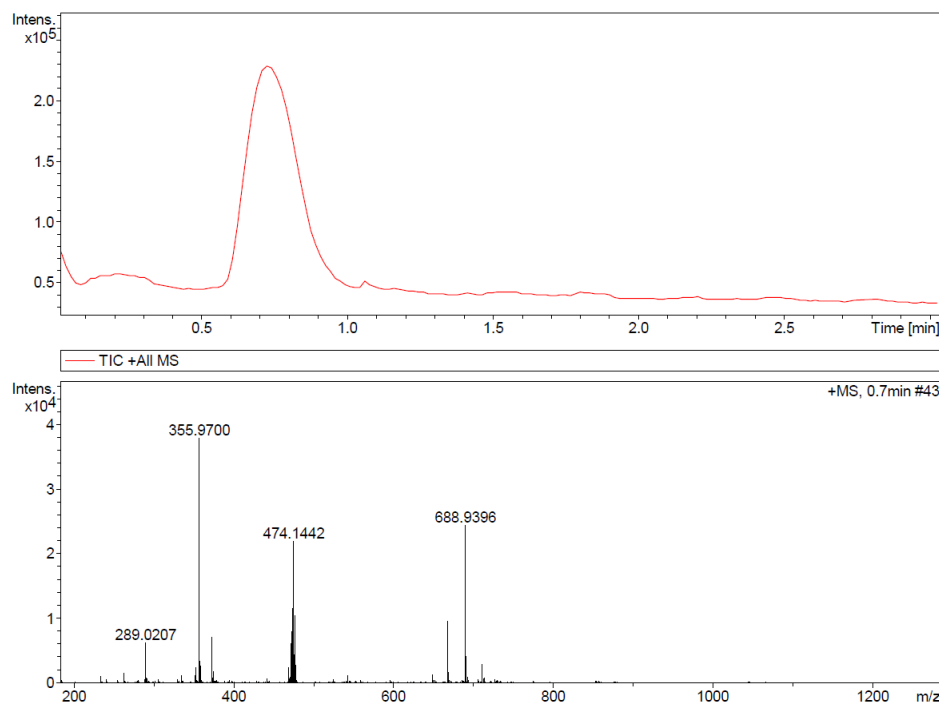


Figure 12: MS(ESI) of 3-((2,3,5,6-tetrafluoro-4-sulfamoyl phenyl)thio)propanoic acid **4**

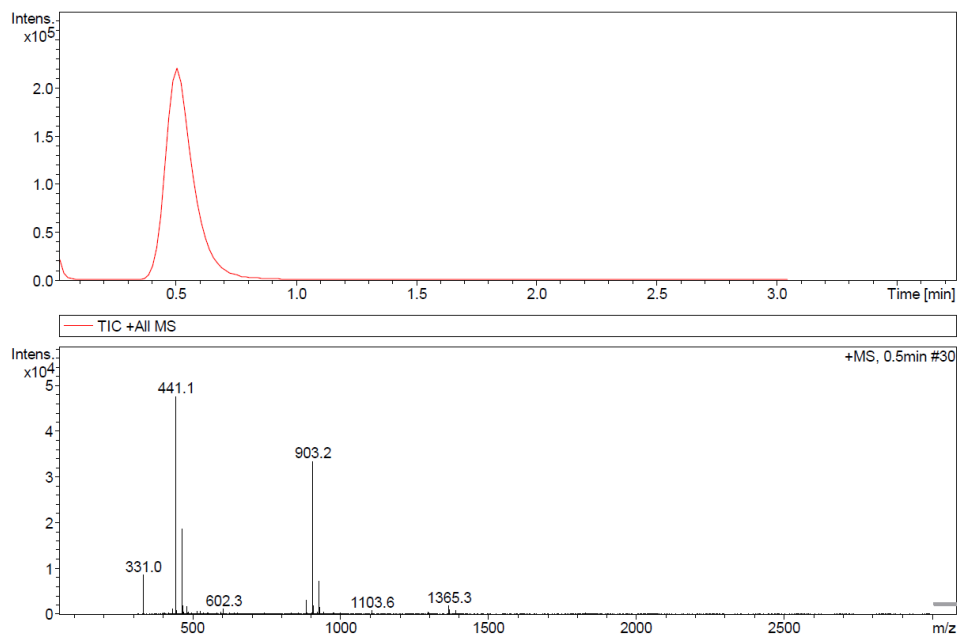


Figure 13: MS(ESI) of 3-((3-(cyclooctylamine)-2,5,6-trifluoro-4-sulfamoylphenyl)thio) propanoic acid **6**

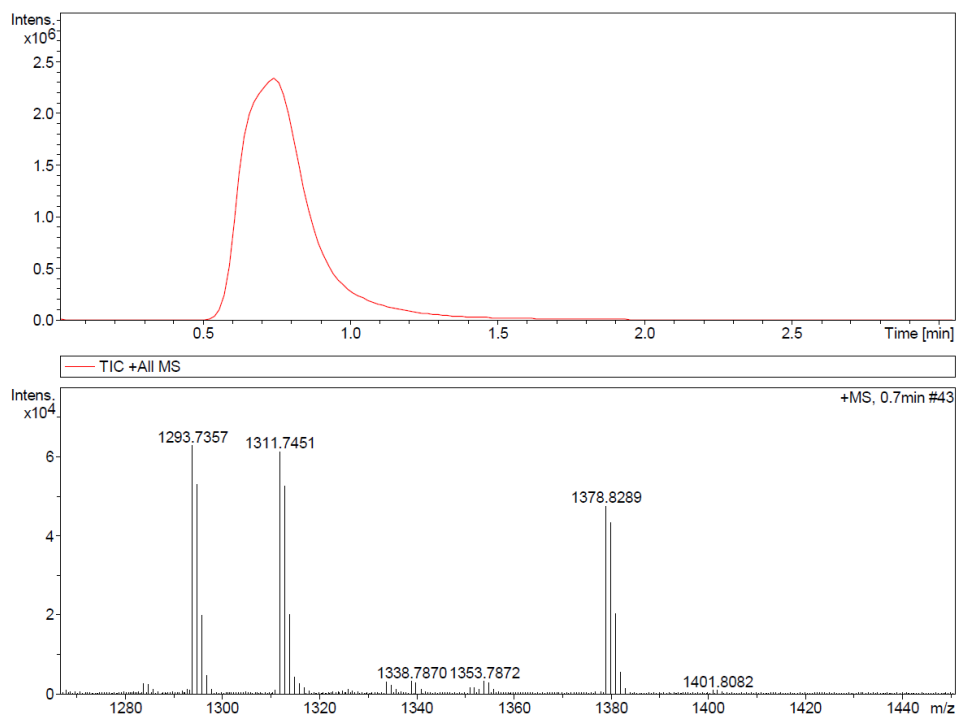


Figure 14: MS(ESI) of CA IX targeted Rhodamine B fluorescent probe **12**

IR Spectra

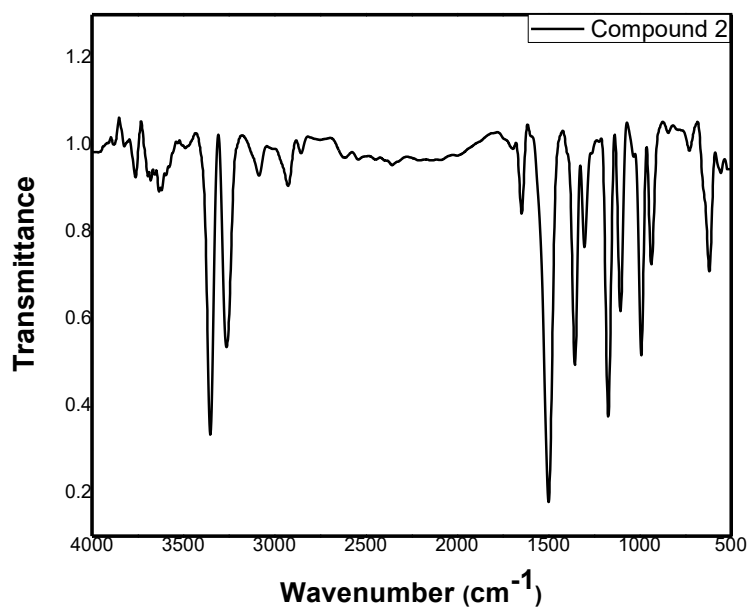


Figure 16: IR spectrum of pentafluorobenzenesulfonamide **2**

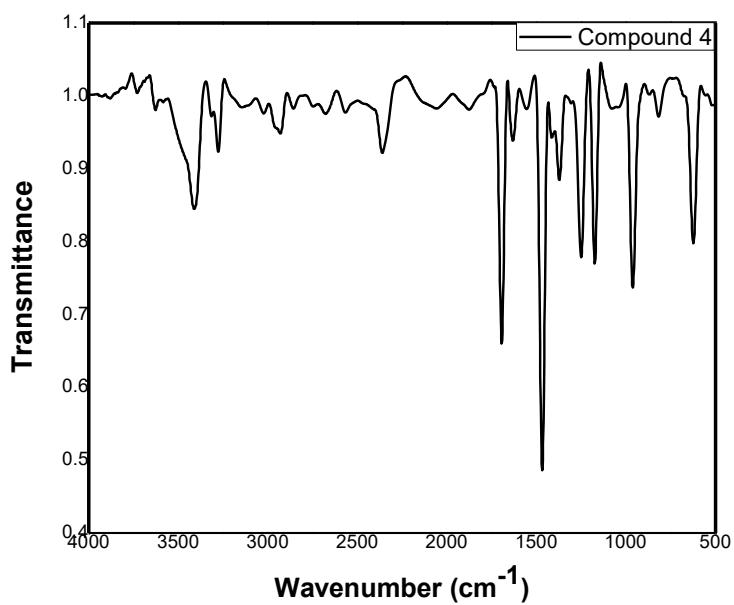


Figure 17: IR spectrum of 3-((2,3,5,6-tetrafluoro-4-sulfamoyl phenyl)thio)propanoic acid **4**

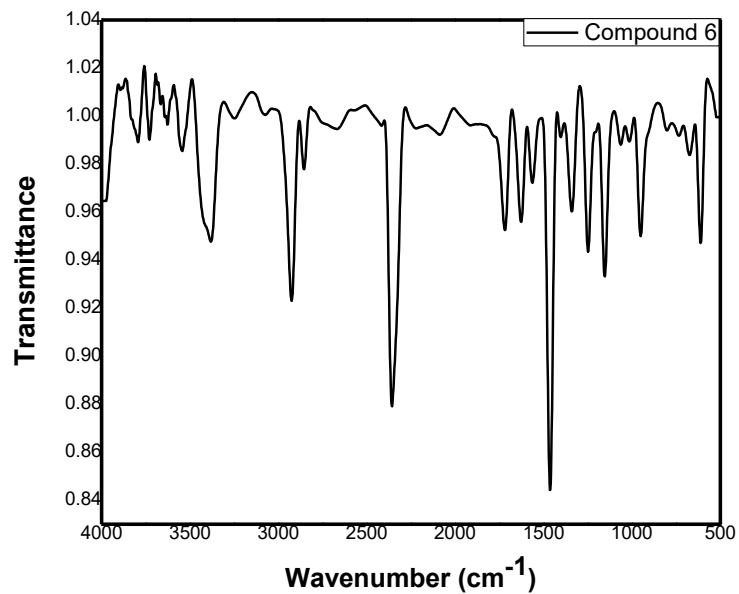


Figure 18: IR spectrum of 3-((3-(cyclooctylamine)-2,5,6-trifluoro-4-sulfamoylphenyl)thio) propanoic acid **6**

REFERENCES

1. Kleihues, P.; Cavanee, W.K. eds: Pathology and genetics. In *tumours of the nervous system, World Health Organization classification of tumours* Lyon: International Agency for Research on Cancer. **2000**, Chapter: Oligodendrogliomas
2. Reifenberger, G.; Louis, D.N. Oligodendroglioma: Toward molecular definitions in diagnostic neuro-oncology. *J. Neuropathol. Exp. Neurol.* **2003**, 62, 111–126.
3. Fortin, D.; Cairncross, GJ.; Hammond, RR. Oligodendroglioma: an appraisal of recent data pertaining to diagnosis and treatment. *Neurosurgery.* **1999**, 45, 1279–1291
4. Jarvela, S.; Bragge, H.; Paunu, N.; *et.al.* Antioxidant enzymes in oligodendroglial brain tumors: association with proliferation, apoptotic activity and survival. *J. Neurooncol.* **2006**, 77, 131–140
5. Järvelä, S.; Parkkila, S.; Bragge, H.; Kähkönen, M.; Parkkila, A.K.; Soini, Y.; Pastorekova, S.; Pastorek, J.; Haapasalo, H. Carbonic anhydrase IX in oligodendroglial brain tumors. *BMC Cancer.* **2008**, **8**:1
6. Haapasalo, J.A.; Nordfors, K.M.; Hilvo, M.; *et.al.* Expression of carbonic anhydrase IX in astrocytic tumors predicts poor prognosis. *Clin Cancer Res.* **2006**, 12, 473–477.
7. Chrastina, A.; Zavada, J.; Parkkila, S.; Kaluz, S.; Kaluzova, M.; Rajcani, J.; Pastorek, J.; Pastorekova, S. Biodistribution and pharmacokinetics of ¹²⁵I-labeled monoclonal antibody M75 specific for carbonic anhydrase IX, an intrinsic marker of hypoxia, in nude mice xenografted with human colorectal carcinoma. *Int. J. Cancer.* **2003**, 105, 873–881
8. Ivanov, S.; Liao, S.Y.; Ivanova, A.; Danilkovitch-Miagkova, A.; Tarasova, N.; *et.al.* Expression of hypoxia-inducible cell-surface

- transmembrane carbonic anhydrases in human cancer. *Am. J. Pathol.* **2001**, 158, 905–919.
9. Zavada, J.; Zavadova, Z.; Pastorekova, S.; Ciampor, F.; Pastorek, J.; Zelnik, V. Expression of MaTu-MN protein in human tumor cultures and in clinical specimens. *Int. J. Cancer.* **1993**, 54, 268–274.
 10. Moulder, J.E.; Rockwell, S. Tumor hypoxia: Its impact on cancer therapy. *Cancer Metastasis Rev.* **1987**, 5, 313–341.
 11. Peskin, B.; Carter, M.J. Chronic cellular hypoxia as the prime cause of cancer: What is the de-oxygenating role of adulterated and improper ratios of polyunsaturated fatty acids when incorporated into cell membranes? *Med. Hypotheses.* **2008**, 70, 298–304.
 12. (a) Krishnan, M. A.; Sengupta, S.; Venkatesh, C. Preparation of ligand targeted drug conjugates for cancer therapy and their evaluation *in vitro*. *Curr. Protoc. Chem. Biol.* **2018**, 50, 1–25. (b) Krishnan, M. A.; Pandit, A.; Venkatesh, C. *In vivo* evaluation of ligand targeted drug conjugates for cancer therapy. *Curr. Protoc. Chem. Biol.* **2018**, 49, 1–21.
 13. Pandit, A.; Sengupta, S.; Krishnan, M. A.; Reddy, R. B.; Sharma, R.; Venkatesh, C. First report on 3D-QSAR and molecular dynamics based docking studies of GCPII inhibitors for targeted drug delivery applications. *J. Mol. Struct.* **2018**, 1159, 179–192.
 14. Rangasamy, L.; Venkatesh C.; Kanduluru, A. K.; Srinivasarao, M.; Bandara, N. A.; You, F.; Orellana, E. A.; Kasinski, A. L.; Low, P. S. New mechanism for release of endosomal contents: Osmotic lysis via nigericin-mediated K^+/H^+ exchange. *Bioconjugate Chem.* **2018**, 29, 1047–1059.
 15. Roy, J.; Nguyen, T. X.; Kandaluru, A. K.; Venkatesh, C.; Lv, W.; Reddy, P.V.N.; Low, P. S.; Cushman, M. Dupa conjugation of a cytotoxic indenoisoquinoline topoisomerase I inhibitor for

- selective prostate cancer cell targeting. *J. Med. Chem.* **2015**, 58, 3094–3103.
16. Poh, S.; Venkatesh, C.; Low, P. S. Comparison of nanoparticle penetration into solid tumors and sites of inflammation: studies using targeted and non-targeted liposomes. *Nanomedicine.* **2015**, 10, 1439–1449.
 17. Poh, S.; Venkatesh, C.; Lindsay, K.; Ayala- López, W.; Balasubramanian, V.; Putt, K. S.; Low, P. S. Folate-conjugated liposomes target and deliver therapeutics to immune cells in a rat model of rheumatoid arthritis. *Nanomedicine (Lond.)*. **2017**, 12, 2441–2451.
 18. Poh, S.; Venkatesh, C.; Ayala- López, W.; Putt, K. S.; Low, P. S. Selective liposome targeting of folate receptor positive immune cells in inflammatory diseases. *Nanomedicine: Nanotechnology, Biology, and Medicine.* **2018**, 14, 1033–1043.
 19. Low, P. S.; Venkatesh, C.; Kim, Y. Prostate specific membrane antigen binding ligand linker conjugates and methods for using...to diagnose and treat prostate cancer. Feb.**2010**, US Provisional Application Serial No.61/308,190.
 20. Low, P. S.; Balasubramanian, V.; Venkatesh, C. Folate receptor alpha targeting ligands. Dec.**2010**, US Provisional Application Serial No.61/428,842.
 21. Low, P.S.; Venkatesh, C. Endosomal escape of biologics (siRNA, peptide, aptamer, protein, gene, etc.) using ionophores in pathological cells. May.**2016**, PCT/US2016/031738.
 22. Seidel, K.; Balakrishnan, A.; Alexiou, C. *et.al.* Synthesis of magnetic-nanoparticle/ansamitocin conjugates-inductive heating leads to decreased cell proliferation in vitro and attenuation of tumour growth in vivo. *Chem. Eur. J.* **2017**, 23, 562–570.
 23. Zee, J. Heating the patient a promising approach? *Annals of oncology.* **2002**, 13, 1173–1184.

24. Kirschning, A.; Kupracz, L.; Hartwig, J. New synthetic opportunities in miniaturized flow reactors with inductive heating. *Chem. Lett.* **2012**, 41, 562–570.
25. Ivanov, S.; Liao, S.; Ivanova, A.; *et.al.* Expression of hypoxia-inducible cell-surface transmembrane carbonic anhydrases in human cancer. *Am. J. Pathol.* **2001**, 158, 905–919.
26. Said, H.; Staab, A.; Distinct patterns of hypoxic expression of carbonic anhydrase IX (CA IX) in human malignant glioma cell lines. *J. Neurooncol.* **2007**, 81, 27–38.
27. Supuran, C. T.; Scozzafava, A.; Conway, J. Carbonic anhydrase-its inhibitors and activators; CRC Press: Boca Raton FL, USA, **2004**. 1–363.
28. Krishnamurthy, V. M.; Bohall, B. R.; Kim, C.-Y.; Moustakas, D. T.; Christianson, D. W.; Whitesides, G. M. Thermodynamic parameters for the association of fluorinated benzenesulfonamides with bovine carbonic anhydrase II. *Chem. Asian J.* **2007**, 2, 94.
29. Dudutiene, V.; Zubriene, A. *et.al.* 4-Substituted-2,3,5,6-tetrafluorobenzenesulfonamides as inhibitors of carbonic anhydrases I, II, VII, XII, and XIII. *Bioorg. Med. Chem.* **2003**, 21, 2093–2106.
30. Dudutiene, V.; Matuliene, J. *et.al.* Discovery and characterization of novel selective inhibitors of carbonic anhydrase IX. *J. Med. Chem.* **2014**, 57, 9435–9446.
31. Krall, N.; Pretto, F.; Decurtins, W.; Bernardes, G.J. L.; Supuran, C.T.; Neri, D. A Small-molecule drug conjugate for the treatment of carbonic anhydrase IX expressing tumors. *Angew. Chem. Int. Ed.* **2014**, 53, 4231–4235.
32. Krall, N.; Pretto, F.; Neri, D. A bivalent small molecule-drug conjugate directed against carbonic anhydrase IX can elicit complete tumour regression in mice. *Chem. Sci.* **2014**, 5, 3640–3644.

33. Marks, I. S., Gardeen, S. S., Kurdziel, S. J., Nicolaou, S. T., Woods, J. E., Kularatne, S. A., & Low, P. S. (2018), Development of a small molecule tubulysin B conjugate for treatment of carbonic anhydrase IX receptor expressing cancers. *Mol. Pharm.*, **15**, 2289–2296.
34. Wong, M.; Zhang, H.; Qin, L.; Chen, H.; Fang, C.; Lu, A.; Yang, Z. Carbonic anhydrase IX-directed immunoliposomes for targeted drug delivery to human lung cancer cells in vitro. *Drug. Des. Dev. Ther.* **2014**, *8*, 993–1001.
35. Cazzamalli, S.; Corso, A. D.; Neri, D. Linker stability influences the anti-tumor activity of acetazolamide-drug conjugates for the therapy of renal cell carcinoma. *J. Controlled Release* **2017**, *246*, 39–45.
36. Lv, P. C.; Roy, J.; Putt, K. S.; Low, P. S. Evaluation of nonpeptidic ligand conjugates for the treatment of hypoxic and carbonic anhydrase IX-expressing cancers. *Mol. Cancer Ther.* **2017**, *16*, 453–460.
37. Stiti, M.; Cecchi, A.; Rami, M.; Abdaoui, M.; Barragan-Montero, V.; Scozzafava, A.; Guari, Y.; Winum, J. Y.; Supuran, C. T. Carbonic anhydrase inhibitor coated gold nanoparticles selectively inhibit the tumor-associated isoform IX over the cytosolic isozymes I and II. *J. Am. Chem. Soc.* **2008**, *130*, 16130–16131.
38. Bellissima, F.; Carta, F.; Innocenti, A.; Scozzafava, A.; Baglioni, P.; Supuran, C. T.; Berti, D. Structural modulation of the biological activity of gold nanoparticles functionalized with a carbonic anhydrase inhibitor. *Eur. Phys. J. E: Soft Matter* **2013**, *36*, 48
39. Touisni, N.; Kanfar, N.; Ulrich, S.; Dumy, P.; Supuran, C. T.; Mehdi, A.; Winum, J. Y. Fluorescent silica nanoparticles with multivalent inhibitory effects towards carbonic anhydrases. *Chemistry* **2015**, *21*, 10306–10309.